INVESTIGATION OF MECHANICAL SEALS

Thesis by

Boris Auksmann

In Partial Fulfillment of the Requirements

For the Degree of

Doctor of Philosophy

California Institute of Technology

Pasadena, California

1964

(Submitted May 12, 1964)

ACKNOWLEDGMENTS

The author wishes to thank Professor Dino A. Morelli for suggesting the research subject and for his help, advice and encouragement. His constructive criticisms and discussions during the apparatus design and the critical review of the manuscript are deeply appreciated.

Thanks are also due to Professor Aladar Hollander for sharing his experience in the mechanical seal research field and for making available his personal reference material.

The author further wishes to express his gratitude to many persons for their assistance during the investigation and the preparation of the manuscript.

Professor Thad Vreeland, Jr. and Mr. Milton J. Wood provided the strain gauges and made available the instruments for readout and calibration. Professor Thomas K. Caughey advised on illumination problems and lent the microflash unit for high speed photography. Messrs. Carl T. Eastvedt and James W. McClanahan advised on photographic techniques and carried out special development and reproduction work. Mr. Donald W. Laird offered many helpful suggestions on manufacturing and machining problems. The personnel in the Mechanical Engineering Shop and the Central Shop did a creditable job in producing the apparatus components. Mrs. Bette N. Shannon typed most of the original and all of the final manuscript.

The author is indebted to the California Institute of Technology for financing this project. During the investigation the author received financial assistance from Institute Graduate Scholarships and Fellowships for which he wishes to express his appreciation.

ABSTRACT

A general description of the mechanical seal problem is given with references to historical background.

The design criteria, establishing the basic configuration, and the evolution of the final design of the experimental apparatus are presented in detail. The description of the supporting equipment and instrumentation is given; calibration curves are included in the appendix. The modifications and suggested improvements in the apparatus are discussed in detail. A complete set of manufacturing drawings for the apparatus that was built and used for the experimental work is on file in the Mechanical Engineering Department of California Institute of Technology; the drawings are not included in the thesis, but prints or microfilm copies are available.

In the experimental work, the qualitative determination of the clearance geometry and the fluid film behavior in the clearance of an operating seal are described. Measured leakage rates and friction coefficients are presented in graphical form together with the pertinent operating variables. Photographs of typical interference fringe patterns and seal face failures at various stages are included.

The sealing mechanism is established and discussed with references to the photographs and numerical data. The usefulness of the balance ratio of a mechanical seal as a basic parameter is

established; the correlation of leakage rates and friction coefficient values with the balance ratio and other operating variables is discussed. The frictional heat rate per unit seal area is shown to be the important criterion for predicting seal failures under different operating conditions. An evaluation of experimental errors is included.

In conclusion a program is proposed for continuation of the experimental work and salient points in the results are summarized.

TABLE OF CONTENTS

LIST OF FIGURES

LIST OF SYMBOLS

D	outer diameter of seal ring	in
d	inner diameter of seal ring	in
$\overline{D}$	average diameter = $\frac{1}{2}(D + d)$	in
$\overline{R}$	average radius of seal ring	in
b	seal face width = $\frac{1}{2}(D - d)$	in
z	seal clearance	in
Δz	axial runout	in
A	seal face area	in^2
P_D	discharge pressure	psig
P_S	supply pressure	psig
P	sealed fluid pressure = $\frac{1}{2}(P_S + P_D)$	psig
	i.e. pressure differential across the seal face	
F	total closure force	lb
N	total force on seal face	lb
$\overline{p}$	average seal face press	psi
S	Shear force at $\overline{R}$	lb
n	rotation speed	rpm
$\overline{v}$	average rubbing velocity	fpm
t	seal supply reservoir temperature	^oF
η	absolute viscosity	lb sec/ft^2
ν	kinematic viscosity	ft^2/sec
ν_t	kinematic viscosity of hydraulic oil at t	ft^2/sec
Q	leakage rate	cm^3/min
β	balance ratio=$\frac{\overline{p}}{P}$	
μ	seal friction coefficient = $\frac{\overline{s}}{\overline{p}}$	
w	weight of the window assembly	lb
r_T	net torque reading	μin/in
r_F	net closure force reading	μin/in
$\overline{s}$	average shear stress on seal face	lb/in^2

I. INTRODUCTION

Over the past 50 years mechanical seals have evolved from specialty items into standard components produced in large numbers. The designs of commercially available seals are many; however, the essential elements in all seal designs are similar. These consist of a flat stationary face and a flat rotating annular face held together by spring and fluid pressure forces. One face is usually made of some hard material while the other face is often made of graphite-carbon impregnated with metal, plastic, metallic salt or some secret proprietary compound.

Although many descriptions of seal designs can be found in the literature, design data either are not available or do not exist, except for the requirements of flatness and surface finish at the seal faces. The required degree of flatness quoted by most investigators and manufacturers is 2 to 3 lightbands per inch*, i.e. curvatures not exceeding 0.00002 - 0.00003 inch per inch.

Available literature reveals that the actual sealing mechanism is not yet understood. There is no valid theory that explains the sealing mechanism which is adequately substantiated by experimental results.

---

* Wavelength of monochromatic light $\lambda \approx 20 \times 10^{-6}$ inch.

In the early papers on mechanical seals A. Hollander[1]* in 1944, and C. E. Schmitz[2] in 1948, both state that the desirable condition for best seal operation is a thin film separating the seal faces. This film may occasionally break resulting in boundary lubrication and some wear. Hollander also refers to boundary film investigations by Needs[3] and other attempts to explain the mechanism that could maintain a fluid film between the seal faces.

Other authors more recently propose different theories involving all possibilities from boundary lubrication[4], through monomolecular layer[5], to full hydrodynamic lubrication[6]. All proposed theories are based on few experimental data, if any, and the unknown fluid film behavior is "tailored" to fit the particular theory.

In short, attempts to formulate a theory on the basis of existing data lead to the following contradictions: Under stationary conditions there is a net closing (spring) force which keeps the seal faces in a solid-to-solid contact resulting in zero leakage. While running, even at high relative face velocities and pressure differentials, good mechanical seals have extremely low wear rates when compared to those obtained in numerous dry wear tests. One might thus conclude that the seal faces

---

*Numbers in parentheses refer to references at the end of the thesis.

are separated by the fluid film, but such a film must then generate sufficient pressure forces to balance the excess closure force. Under running conditions, a mechanical seal should then behave as an inherently stable thrust bearing. However, according to existing hydrodynamic thrust bearing theories, an axial force cannot be developed between flat faces. Furthermore, all thrust bearings involve substantial radial flow, while good seals have very low leakage.

Modifications of different thrust bearing solutions have been tried by assuming possible distortions in flat seal faces, misalignment, etc., but results are speculative and offer no satisfactory explanation of the sealing mechanism. Effective thrust bearing solutions require angular clearance variations to create load supporting wedges, but such clearance geometry is hardly compatible with carefully lapped and mounted optically flat faces. Clearly, if the nature of the fluid film between seal faces were known, the sealing mechanism could be analyzed without speculation. Combined with additional experimental data it should be possible to arrive at a theory that can be used as a practical design basis.

To obtain needed experimental data it was decided to design and build a special apparatus where the behavior of the fluid film could be visually observed and photographed, while the seal is operated under controlled conditions and with sufficient instrumentation for collecting numerical data.

II. DESIGN OF EXPERIMENTAL APPARATUS

2.1 Design Criteria

In order to establish the design criteria for the apparatus, a survey of commercially available seal designs was carried out. Based on this study it was decided to design the apparatus to satisfy the following basic requirements:

1. One of the seal faces must be transparent to permit observation and photography of the fluid film in the seal clearance.
2. Provisions for measuring torque and closure forces acting on the seal faces under controlled operating conditions must exist.
3. Seal sizes 2 to 5 in.O. D. should be possible.
4. Capacity to maintain differential pressures across the seal up to 500 psig.
5. Speed control over the range of 700 to 4000 rpm should be provided if possible.
6. Easy access to the test seal components for inspection, changes and relapping is desirable.

The reasons for these specifications were:

1. The main object is the investigation of the oil film behavior and the sealing mechanism, rather than determination of the operating limits of the mechanical

seals. Therefore, specifications should include a sufficient range of common sizes and operating conditions but not the extremes.

2. Small seal sizes, although common, are not suitable for visual observation and photography.
3. Preliminary design studies showed that the above requirements would already present challenging design problems. Designing for extreme operating conditions would not be justified in view of the main objective.
4. Design studies indicated that exceeding the chosen specifications by significant amounts would lead to designs that would make the apparatus impossible to build at a reasonable cost.
5. Chosen specifications would allow good use of existing equipment and laboratory facilities for auxiliary services and instrumentation, resulting in considerable savings.

As the actual design of the apparatus progressed other reasons became apparent. These will be mentioned later with the discussion of the apparatus and its design.

2.2 Basic Configuration

The basic configuration of the final design evolved from four requirements that were considered essential and therefore should not be compromised if at all possible. The following is

an account of the design restraints imposed by these four requirements, and how the basic design configuration finally evolved as a compromise between many practical design limitations.

1. Provision for viewing and photography - The observation and successful photography of thin fluid film phenomena depends on achieving sufficient contrast by choosing suitable illumination and the best viewing angle. The difficulties of this task were well-known from an earlier investigation of oilfilm behavior in journal bearings[7]. Thus, to avoid as many lighting, reflection and view obstruction problems as possible, it was decided to keep a large hemispherical space on the outer side of the transparent seal member completely free of all structure. This effectively meant that all available design space was on one side of the observation window.

2. Seal friction torque measurement - Order of magnitude calculations, using available seal friction data, indicated that torques to be measured would, under some operating conditions, be comparable to the parasitic torques in the apparatus. Consequently, designs without provision for isolation of seal friction torques were not acceptable. The two possible alternatives to consider were either to measure friction drag of the rotating face or the reaction torque of the stationary face; the latter, of course, would present fewer instrumentation problems.

3. Alignment of seal faces - In most commercial seal designs the alignment between the seal faces is achieved by mounting the rotating face on a flexible support. The rotating face then finds its own axis of rotation in relation to the fixed face, and thus compensates for the runout in the drive shaft. The closure force is determined by spring preload and fluid pressure. Such a configuration is not easily adaptable for producing a variable closure force that could be closely controlled and measured. If the stationary face were fixed, the measurement of torque would have to be done the hard way through the rotating half; this is not a good solution in any circumstance.

Floating the stationary face on a hydrostatic bearing was considered and discarded as a risky solution. A misaligned or flexibly mounted rotating face running against a stationary face resting on such a support can lead to unstable vibrations which are difficult or impossible to damp out. Any such structure would probably obstruct some of the space needed for viewing the seal faces. After trying several configurations, it became clear that the self-aligning feature of commercial seal designs had to be compromised in order to resolve the torque and closure force measurement problems in a reasonable manner.

In order to eliminate the need for self-alignment the axial shaft runout had to be reduced to a minimum. Thus the basic configuration had to provide a precision spindle with all the necessary

supports and some adjustment to compensate for random errors inevitably associated with machining tolerances. It was estimated that with proper design the maximum axial runout at the test seal face would not exceed 0.0001 inch; this is an order of magnitude lower than that found in commercial seal applications.

Even with this small runout, the unrestrained closure of the seal faces cannot be guaranteed unless the axial closure force is applied free of any moments. The above basic configuration must therefore provide a pivot for the stationary face. The resulting advantage from this trade-off is that, by proper design, such a pivot can also be utilized to isolate the reaction torque of the stationary face for measurement purposes.

4. Controlled closure force - A hydraulic or pneumatic cylinder with a controlled pressure supply is one of the simplest ways to produce a continuously variable force, particularly if no motion is required. The hydraulic loading system also has the advantage that the spring constant, i.e. "hardness", can be varied by adding an accumulator to the system. In this case the deciding factor for a hydraulic loading system, in preference to other possibilities, was the availability of a laboratory hydraulic test stand. The pressure in a hydraulic cylinder, however, is not an accurate measure of the force. Consequently, the convenience and simplicity of the loading system had to be paid for by providing means for accurate closure force measurement in the basic configuration.

5. Other design considerations - In commercial seal designs the preferred arrangement is for radially inward leakage. The primary reason for this is to keep the relatively weak carbon seal in compression. The argument of using the centrifugal force to oppose leakage is also often used. However, numerous broad generalizations and contradictory statements[4] can be found in the technical literature, indicating that centrifugal force effects on the fluid between the faces of a seal are not known. It is also clear that the centrifugal forces are trivial compared with viscous forces in the narrow clearances.

Attempts to conceive a basic configuration with inward leakage and a stationary transparent seal member all failed. Such configurations required giving up at least one of the four essential test apparatus requirements. Inverted configurations with a rotating transparent seal face were also tried but no satisfactory solutions could be found. Even by relaxing the essential requirements all conceivable configurations with inward leakage still ended up with some inherent design problems which were best avoided.

On the other hand several basic configurations with radially outward leakage paths had been conceived and developed in some detail. These appeared feasible and could be worked into a final design satisfying at least the essential experimental requirements.

All these configurations used a vertically mounted spindle to eliminate gravity effects. They could be divided into two types:

a. Single configurations - the main advantages are availability of all space on one side of the stationary transparent seal member, direct measurement of all variables and accessibility to the other end of the spindle for drive, cooling, closure, instrumentation, etc. The main disadvantages are large closure loads carried by the spindle and the bearings thus requiring a large and rigid structure. The friction losses in large, heavily loaded spindle bearings are appreciable; hence, cooling for the bearings becomes a necessity.

b. Back-to-back configurations - the advantages are low spindle bearing loads allowing use of smaller bearings, lighter apparatus structure, and operation without special cooling for the spindle bearings. The disadvantages are, either matching two test seals, or isolating these torsionally from each other without losing the advantage of the balanced closure. The control and measurement devices for the closure forces, provisions for the circulation of sealing fluid, and the spindle drive are more difficult to design because neither spindle end is easily accessible.

Decision in favor of the basic configuration with a single test seal was made on the basis of relative cost estimates for the two configuration types.

The total cost of supporting structure and auxiliary apparatus components made of common engineering materials depends primarily on the number and the accuracy of the required machining operations, while the cost of the raw material is a relatively small fraction. Therefore, no decisive machining cost differences could be found in favor of either configuration.

The most expensive single components in the apparatus are precision spindle bearings and glass or quartz windows making up the transparent seal member. The cost of a set of large Class 00 roller bearings (runout < 75 parts per million) was found to be 5 to 10 times the cost of a plate glass window, and comparable to the cost of a quartz window. On the other hand the cost of Class 0 bearings (runout < 150 parts per million) is comparable to that of a plate glass window.

If the cost of small bearings for a back-to-back arrangement with a pair of matched test seals was assumed to be negligible, the costs of the two configuration types would be comparable using quartz windows and Class 00 bearings, or using plate glass windows and Class 0 bearings. It was also reasonable to assume that the frequency of window scoring in the back-to-back configuration would be twice that of the single seal configuration. In such case the cost breakeven point for the Class 00 bearings and plate glass window combination would be reached after a few scorings of the

windows. Thus with or without the need for quartz windows a single test seal configuration appeared favorable except for a very short test program.

The final compelling reason for a single seal configuration is the time required for lapping the mechanical seal faces to the required degree of flatness and surface finish. It was found that, depending on the seal material and the initial surface quality, the lapping of one seal face may take from a quarter of an hour up to two hours. When additional requirements have to be met, such as matching two seals, the lapping time will be considerably longer.

In view of all the foregoing arguments, the selection of a single test seal configuration for the apparatus is considered well justified by this writer.

2.3 Detailed Design

A sectional and an isometric view of the final detailed apparatus design are shown in Figures 1 and 2, respectively. The exact shapes, dimensions and materials of each single component listed in Figure 1 were determined on the basis of design calculations for strength and rigidity, with due consideration of availability of materials, machining operations and overall cost.

For the largest seal size of 5 inches O.D. and maximum sealed pressure of 500 psig, the spindle, supporting structure, and the load measuring mechanism had to be designed for 8400 pounds maximum force.

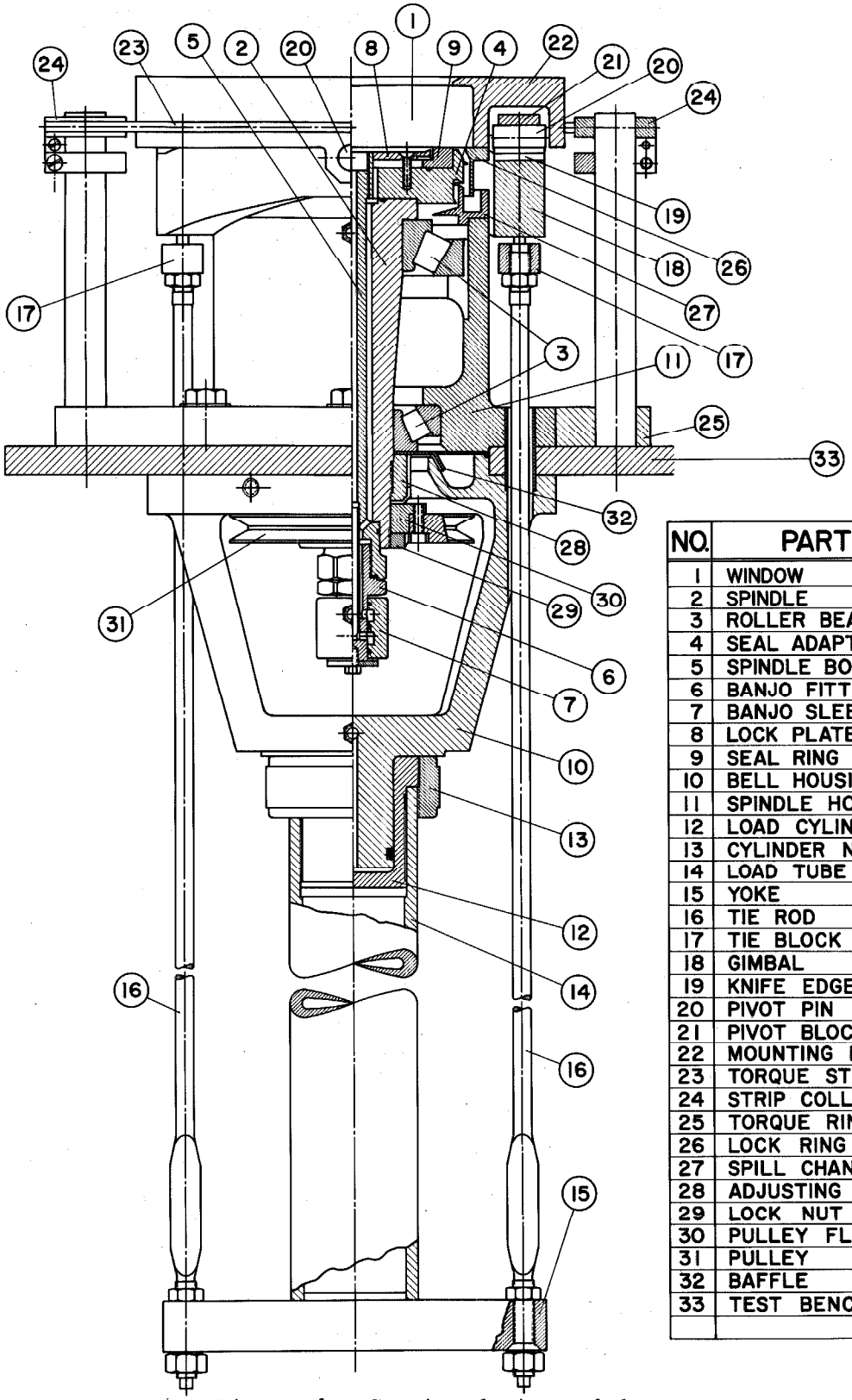

NO.	PART	DWG.
1	WINDOW	14
2	SPINDLE	9
3	ROLLER BEARING	
4	SEAL ADAPTER	10
5	SPINDLE BOLT	8
6	BANJO FITTING	6
7	BANJO SLEEVE	7
8	LOCK PLATE	13
9	SEAL RING	12
10	BELL HOUSING	1
11	SPINDLE HOUSING	2
12	LOAD CYLINDER	22
13	CYLINDER NUT	23
14	LOAD TUBE	21
15	YOKE	20
16	TIE ROD	19
17	TIE BLOCK	18
18	GIMBAL	4
19	KNIFE EDGE	15
20	PIVOT PIN	15
21	PIVOT BLOCK	17
22	MOUNTING RING	3
23	TORQUE STRIP	
24	STRIP COLLAR	29
25	TORQUE RING	24
26	LOCK RING	5
27	SPILL CHANNEL	11
28	ADJUSTING NUT	25
29	LOCK NUT	27
30	PULLEY FLANGE	26
31	PULLEY	
32	BAFFLE	
33	TEST BENCH	28

Figure 1. Sectional view of the apparatus.

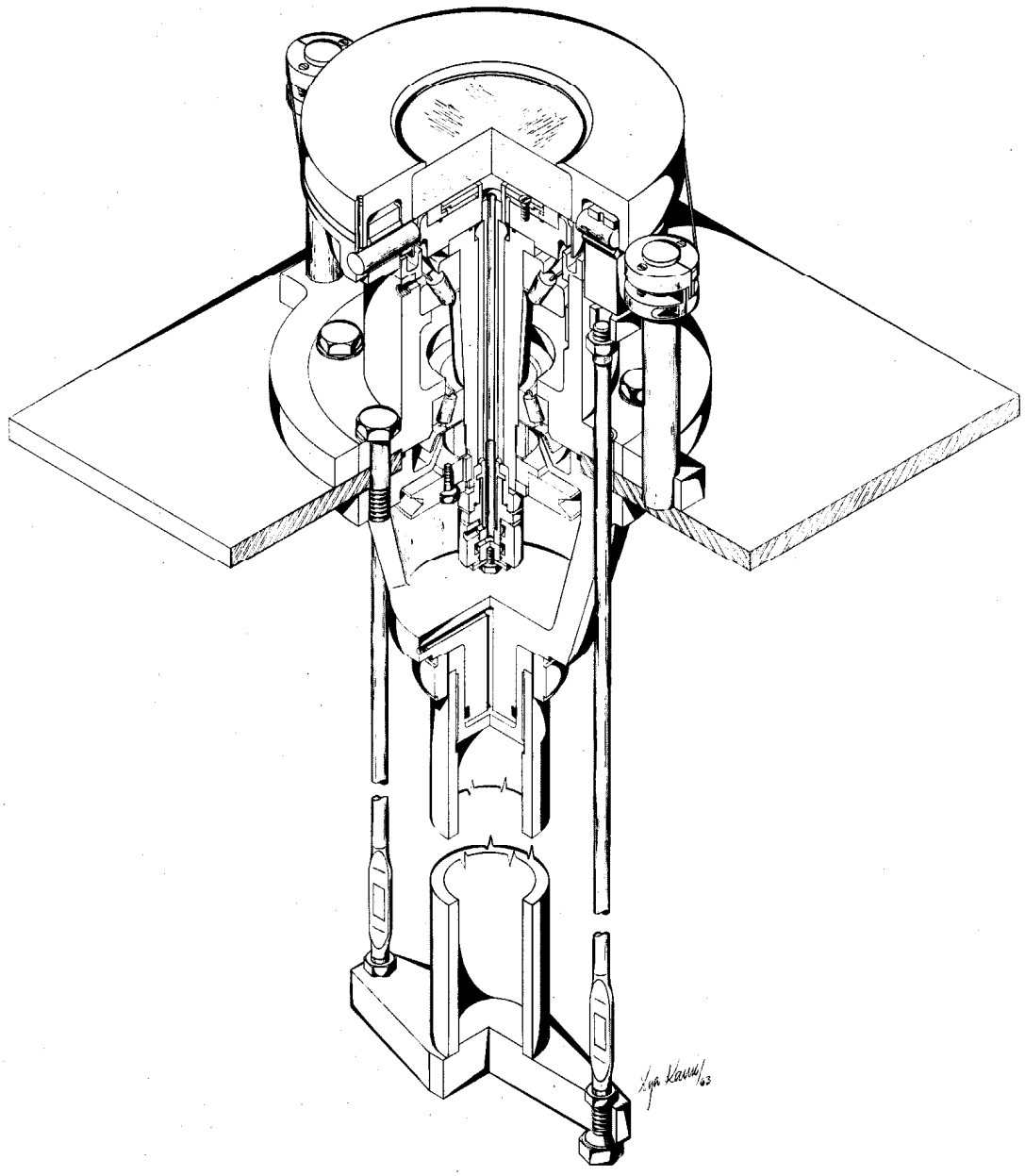

Figure 2. Isometric view of the apparatus.

Plate Glass Window [1] *. Observation of the fluid film between the faces of the test seal is through the transparent stationary half of the seal which is in the form of a round plate glass window. On the basis of the maximum recommended tensile working stress of 2000 lb./in.^{2} for tempered plate glass, the required window thickness is 1.5 inches. With full design load the maximum deflection in the center is about 0.001 inch. Deflection varies as the second power of the radius, so the maximum slope in the vicinity of the face of a 5 inch O.D. test seal is of the order of 0.0005 inch/inch. This means that due to the deflection of the glass alone one would expect a clearance variation of the order of 250×10^{-6} inches over a seal face width of 1/2 inch. This corresponds to more than 20 light bands (using light of 5875.6 Å wavelength).

It also became obvious that this distortion could not be significantly reduced. The elastic modulus of fused quartz is 12×10^6 lb./in.^{2} as compared to 9×10^6 lb./in.^{2} for plate glass, i.e. a reduction of distortion by some 30 per cent. Increasing the thickness of the window appears to be the most effective way of reducing distortion since deflection varies inversely with the third power of thickness. However, to keep the distortion within

---

* Numbers in brackets refer to components in Figure 1.

the limits of accepted flatness specifications requires a reduction of distortion by an order of magnitude. A window 2.16 times thicker or about 3 inches thick would be required. Such a window thickness drastically limits the field of view and results in bad lighting problems, defeating the main purpose of the investigation. Plate glass windows 1.5 inches thick and 6 inches in diameter could be procured at a reasonable cost ($35 apiece), while a 3 inch thick window is much more costly and difficult to obtain.

In most practical installations mechanical seals are supported by much more flexible structures than this test equipment; it became clear that finer flatness standards under operating loads would hardly simulate an actual mechanical seal in operation. It was decided to use a 1.5 inch thick window and limit deflections by operating the largest seals at lower pressures. With high pressures smaller size seals would be mandatory if distortions turned out to be objectionable.

This compromise gave a limited means for controlling the distortions and, incidentally, also gave some means for examining the effect of distortions on the sealing mechanism.

Precision Spindle [2] and Bearings [3] . For a precision spindle a preloaded bearing arrangement is essential. The top bearing was selected on the basis of the maximum load and 1000 hour life at 4000 rpm. The bottom bearing carries only the preload forces and could be very small; however, in this case the size

was dictated by the minimum spindle diameter to accommodate two passages for the circulation of the liquid to provide cooling and controlled pressure at the seal faces.

In the spindle design special consideration had to be given to manufacturing problems. For precision grinding of bearing seats and the seal adapter [4] seat, provisions for false centers were included at both ends. To provide hard bearing seats (Rockwell C30-35) without heat treating and subsequent finish machining, the spindle was designed for machining directly from hardened steel. The double passage complications were effectively shifted to the spindle bolt [5] , and banjo fitting [6] , which were easier to machine and required less precision.

Careful consideration of the grinding tolerances also indicated that Class 0 bearings can be used without increasing the spindle runout significantly. In particular, grinding tolerances of $\pm$ 0.00005 inch can be and are produced by commercial grinders at reasonable prices. With effective bearing centers 6 inches apart and Class 0 bearings (runout < 0.00015) the axial runout of the seal adapter seat periphery would be in the worst possible case less than 0.000075 which is of the same order as grinding tolerances. Seal adapter [4] machining tolerances for face parallelism would also be of the order of $\pm$ 0.0001 inch and considerable compensation can be achieved by selective orientation in assembling these parts.

Thus Class 00 bearings, which have twice the precision and about five times the cost, would be wasted. In addition to the lower cost the delivery time for Class 0 bearings was shorter by several months.

The double banjo sleeve [7] for the hose connections to the seal fluid circulation passages in the spindle is designed with minimum possible diameter in order to reduce the rubbing velocity of the rotary O-ring seals. The double arrangement uses only two high pressure seals, the third seal in the middle is subject to differential pressure only. Having all O-rings of equal size eliminates the end thrust problem; and incidentally, reduces the number of O-ring sizes to be stored for replacing the worn ones.

At the top end of the spindle the seal ring lock-plate [8] is designed to provide uniformly distributed flow radially outward, upward past the seal ring, and radially inward along the window for return through the central passage in the spindle bolt [5] . In the design of the fluid circulation passages it was attempted to maintain a constant effective cross-section so that both supply and return paths would have equal pressure drops.

Supporting Structure. The bell housing [10] and the spindle housing [11] form the structural backbone of the apparatus. The basic shapes of these components, together with the strength and rigidity requirements, made it obvious that they should be designed as castings. Since complex shapes add little to the casting costs,

several useful features were incorporated and ease of assembly was carefully considered in designing these parts. In particular, the bridge member of the bell housing was designed to permit changing of the drive pulleys [31] and banjo fitting O-ring seals without disassembly of other components; a spill groove for collecting the bearing cooling oil was included, and the piston of the hydraulic load cylinder [12] was made integral with the bridge portion of the bell housing. The alignment of the bell housing [10] with the spindle housing [11] is through tubular dowels and independent of the test bench.

The entire apparatus is mounted on a blanchard ground steel plate [33] which forms the top of the test bench. The mounting is designed so that the spindle housing assembly can be dismantled without disturbing the bell housing and vice-versa.

The test bench also serves as the supporting frame for the electric motor to drive the spindle.

Closure Force and its Measurement. The closure force is supplied and controlled by the hydraulic pressure in the load cylinder [12] . For a "soft" system the cylinder is left floating on the hydraulic pressure; an essentially constant force system may also be obtained by connecting an accumulator with an air reservoir into the system. For a "hard" system the loading cylinder nut [13] can be tightened up and the hydraulic pressure may be released. The

spring constant is then governed by the combined elasticity of the tie rods [16] and the loading tube [14] . The long tie rods serve to separate the closure forces from the frictional forces acting on the glass seal member. By proper adjustment of the length of the torque strips [23] , the tie rods [16] can be made perpendicular to the seal face; the friction torque is then carried only by the torque strips [23] .

The yoke [15] is designed to center the loading tube between the tie rods; these in turn are accurately positioned in the yoke by closely fitted tapered nuts and matching seats. The yoke is set perpendicular with respect to the loading tube by adjusting the lengths of the tie rods and checking with a level, or feeler gauges. Since the loading tube is aligned with the bell housing, the tie rods are thus located symmetrically with respect to the spindle axis.

The aluminum load tube [14] acts as a spacer. A heater is installed inside this tube (not shown on Figures 1 and 2) so that the thermal expansion of the long tube can be used to produce a very slow variation of the closure force when the stiff closure system is used. The estimated thermal loading effect with the system resting on the load cylinder nut [13] , is of the order of 20 pounds per degree Fahrenheit temperature rise. To avoid excessive heat loss through the load cylinder, it is made of stainless steel and

the contact area with the aluminum tube is reduced to a minimum; space is also available for insulating washers at both ends of the load tube.

The closure forces are measured directly by strain gauges attached to the flat ground portions near the bottom ends of the tie rods. There are four strain gauges on each rod mounted on opposite sides to provide compensation for bending and thermal effects; all are connected into a common bridge circuit to read total force directly.

In the early design stages, the measurement of closure force by direct weighing was also considered. To do this with sufficient accuracy the radius of the balance knife edges must be small compared to the shortest lever arm in the balance; considering the physical size of the apparatus, even compound levers with more than 100 to 1 overall ratio would be impractical. Assuming the shortest lever of 1 inch length and using "Tantung" tool bit with 0.025 inch radius for the knife edge (350,000 psi compressive strength), the required knife edge length to weigh the design load is about 2.5 inches. Any balance structure to back up two such knife edges, i.e. load and reaction pivots, would be rather cumbersome and out of proportion with the rest of the structure.

On the other hand a full gimbal [18] with two such knife edges [19] at right angles turned out to be the practical solution to the pivot for eliminating all moments from the closure force.

Standard 1/4 inch square "Tantung" tool bits are used for knife edges [19] and 5/8 inch round bits for the seats [20] ; total initial cost is less than $10. The only machining operation involving precision is grinding the groove into the round bit; this can be done on an ordinary surface grinder with a profiling attachment for dressing the wheel to the desired radius. Setting both knife edges into the gimbal ring, the pivot axes could be made coplanar within the machining accuracy (i.e. about $\pm$ 0.001 inch). By adjusting the window position with shims so that the face lines up with the seat line of the pivot pins [20] in the mounting ring [22] , the plane of the gimbal axes can be made to coincide with the plane of the seal face. This ensures that any tilting of the glass to follow the rotating seal face can take place without lateral shifting. This design gave a positive closure with a good quality pivot and also provided quick access to the test seal. To remove the window it is necessary only to disconnect the torque strips [23] from the mounting ring [22] , back off the setscrews and pull the two pivot pins [20] . The mounting ring can than be lifted off without disturbing the rest of the apparatus. In actual tests this feature was extremely useful because seal rings [9] could be removed for relapping within a few minutes.

The complex shape of the mounting ring [22] resulted from the need for rigidity in this part as well as in the gimbal ring [18] . Since deflections are proportional to the cube of the span and

inversely proportional to the moment of inertia of the cross-section (i.e. the cube of the height of cross-section) any increase in the diameter required a proportional increase in vertical direction. The only solution to this unfortunate condition was to nest the gimbal ring [18] inside the mounting ring [22] , which also gave the best support for the knife edge pivot pins.

Torque Measurement. As already mentioned the glass window is held against the seal ring by the closure force supplied through long tie rods [16] , the gimbal [18] and the mounting ring [22] .

The seal friction is measured directly in terms of the reaction torque required to hold the mounting ring stationary. This reaction torque is supplied by two flexible steel strips [23] connecting the mounting ring [22] to the torque strip collars [24] . The torque strips [23] are made from standard 0.002 or 0.001 inch feeler gauge stock which is readily available. One of the strips is equipped with four strain gauges forming a temperature compensated bridge, and is calibrated for direct force readout.

The accuracy of the torque measurement is dependent on careful separation of the reaction torque from the closure forces, and on the proper alignment of the mounting ring with the axis of the spindle. The design provisions to eliminate the external moments and torque loads, by the long tie rod and full gimbal arrangement, have been discussed in the preceding section. For aligning the center of the mounting ring with the spindle axis further adjustments are provided in the design.

The spindle housing flange is used as a pilot to center the torque ring [25] ; this positions the torque strip collars [24] symmetrically with respect to the spindle axis. The mounting ring [22] is then centered over the spindle by individual adjustment of the torque strip lengths with the screws in the collars [24] . A second set of screws in the collars provides for fine adjustment of the torque strip ends in the vertical direction. Once this adjustment is done, the entire window assembly can be rotated about the spindle axis by turning the torque ring. This rotation is used to adjust the perpendicularity of the tie rods in the tangential direction.

One of the gimbal axes is fixed in the mounting ring by the pivot pins; the gimbal is positioned along this line by gauging the space between the pivot pin lugs and the gimbal on both sides. The alignment of the closure is completed by centering the pins [20] in the pivot blocks [21] and setting the ends even with the ends of the knife edges in the gimbal. To check the alignment, the glass window is floated hydrostatically on the supply pressure and allowed to find its own equilibrium position over the stationary spindle; this is also done when establishing the zero reading for torque measurement.

Leakage Measurement. Two labyrinth seals are used to collect the test seal leakage and keep it separated from the cooling oil circulated through the spindle bearings. The first labyrinth is

formed by the slinger near the top of the seal adapter [4] , and the skirt of the lock ring [26] , extending into the spill channel [27] . Because the general arrangement is such that the spill channel is necessarily located inside the gimbal, the drain piping connections to the spill channel created an unusually difficult design problem. Rather than enlarge the gimbal to provide the needed clearance, the gimbal was designed with a special vertical profile to accommodate the drain piping. The advantages of such design were considered well worth the increased cost for machining the gimbal. The drain piping is designed for gravity flow from the spill channel directly into a graduated glass cylinder.

The second labyrinth seal is designed to keep the bearing cooling oil out of the spill channel for the seal leakage. The labyrinth consists of a baffle inside the bore of the spill channel [27] and another slinger ring at the lower edge of the seal adapter [4] .

The use of lip seals was carefully avoided throughout the apparatus design because, at high surface speeds, the friction losses become prohibitive; a bigger and more expensive drive would be needed and other complications may result if additional cooling becomes necessary.

2.4 Auxiliary Equipment.

Hydraulic System. The auxiliary hydraulic system consists of three independent hydraulic units. Two are used to control the

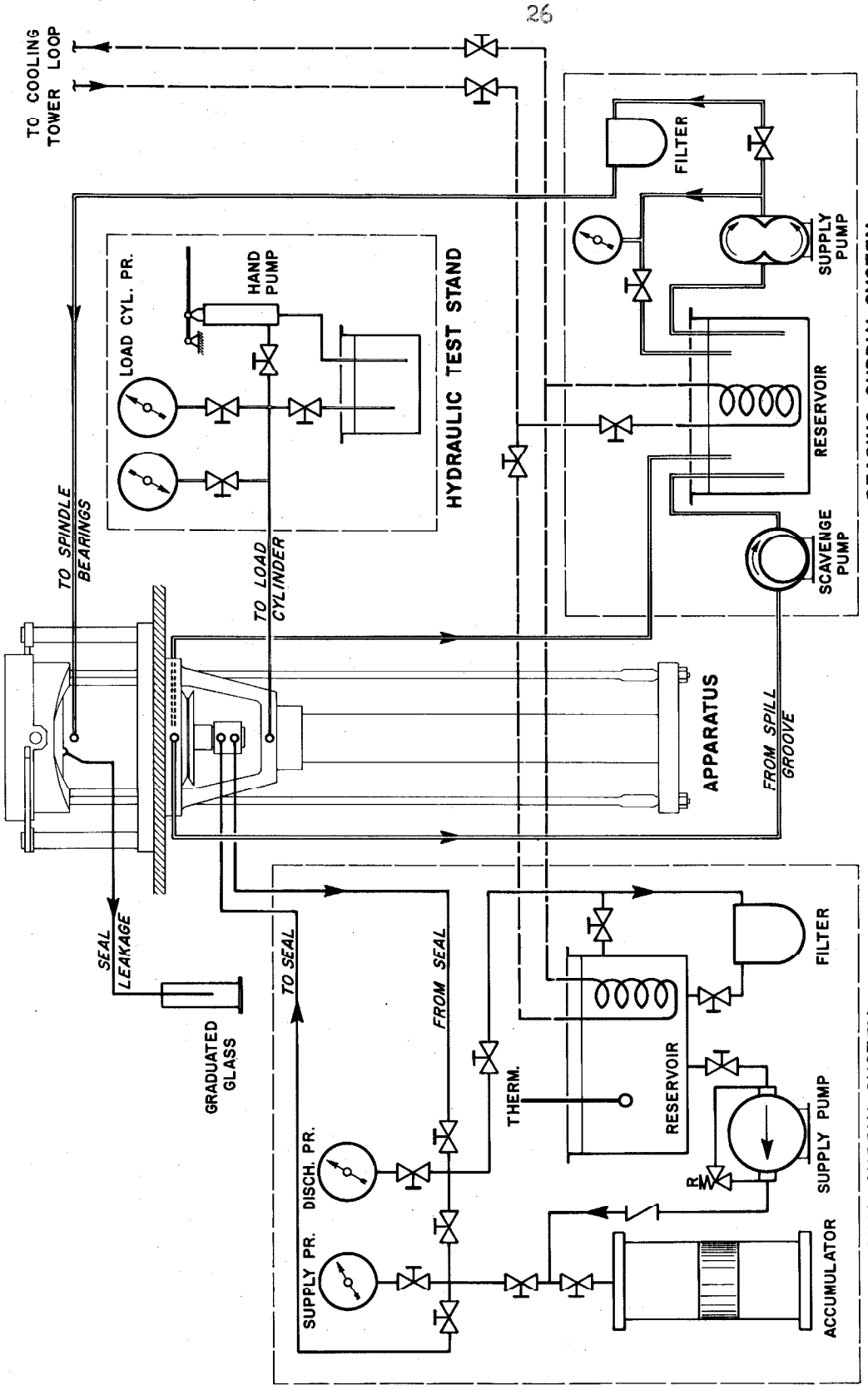

Figure 3. Schematic representation of the auxiliary hydraulic system.

variables in the test seal under operating conditions; the third supplies oil to the spindle bearings. The schematic representation of this entire hydraulic system is given in Figure 3.

The loading cylinder is supplied by a hand pump in the laboratory hydraulic test stand. A shutoff valve is used to confine the pressure in the loading cylinder when the desired load is reached. Two bourdon gauges covering the pressure ranges 0 to 600 psig and 0 to 5000 psig are used to monitor the pressure in the load cylinder.

In the first series of tests hydraulic oil was used as the fluid in the test seal. It was possible to use an existing hydraulic supply unit built by the Dennison Company with only minor modification. A cooling coil had to be installed in the reservoir to control the seal fluid temperature. Two throttling valves in series are used to adjust the supply and discharge pressures fed to the double banjo joint at the lower end of the spindle. Essentially, this allows one to control the pressure at the seal and the differential pressure governing the flow rate past the seal to provide cooling. Additional flow rate control is possible by changing the output rate of the pump in the hydraulic unit. The piston-accumulator in the hydraulic unit is used to reduce pump pulsations and other surges in the system.

Oil for lubrication and cooling of the spindle bearings is supplied by a small gear pump, the pressure being controlled by a

throttled bypass. The bypass flow is utilized to provide circulation around the cooling coil in the oil reservoir. The oil to the bearings is passed through a ceramic filter and is delivered at the periphery of the top spindle bearing by two diametrically opposite taps. The oil runs through both spindle bearings by gravity; any excess oil that cannot pass through the top bearing flows through two bypass passages provided inside the spindle housing at 90° to the supply taps. After passing through the bottom bearing the oil is collected in the spill groove and returned to the reservoir by a scavenge pump and by gravity.

Cooling System. Cooling water for the heat exchange coils in the oil reservoirs is tapped directly from the supply mains in the laboratory.

Spindle Drive. In order to design the spindle drive, and select a suitable electric motor, the power requirements based on the friction losses in the test seal had to be estimated. Some twenty papers on mechanical seals were checked for seal friction data; only two of these (4) and (8) by Mayer contained applicable friction coefficient values. However, the values of $\mu = 0.005$ to 0.1 and $\mu = 0.05$ to 0.15 for low and moderate wear rates respectively represent too broad a range to permit any reasonable estimate of power requirements.

Clearly, if the transparency of the glass window was to be maintained, very little wear and scoring of the glass window could

be tolerated. Thus a value of $\mu = 0.05$ appeared to be reasonable design maximum, particularly if a fluid with good lubricating properties were chosen. To satisfy the maximum design criteria the power requirements would be 1.2 to 12 hp for a friction coefficient range of $\mu = 0.005$ to 0.05. Since the available friction data is so limited and widely scattered the above figures are very unreliable. Rather than be committed to the expenses of buying a 12 hp motor and the necessary controls, it was decided to experiment with a smaller motor. By starting out with smaller seals and lower speeds, considerable data could be obtained. If a more powerful drive should become necessary, there would be enough data to determine the exact requirements.

The drive was designed for a single 3/8 inch V-belt, commonly known as a 3V cross-section, with a maximum power transmission capacity of about 8 hp at the spindle speed of 4000 rpm. To cover the contingencies a provision was made to accommodate a two groove pulley if necessary.

A 1.5 hp compound wound D.C. motor was available at a very low cost and it was decided to use that motor for the initial experimental program. By utilizing both the 125 V and 250 V D.C. supply in the laboratory, and controlling both armature and field voltage with variable resistors, spindle speed variation of nearly 50 per cent could be obtained within the range of a single pair of pulleys.

Instrumentation. Since most operating parameters can be measured directly, only a few simple instruments are needed. Both closure and torque forces are measured by temperature compensated strain gauge bridges, which are mounted directly on the apparatus components, designed specifically for strain gauge application. The tie rods were calibrated individually and together in a tensile testing machine. The torque strip was calibrated in the installed position by hanging weights on a fish line using a small ball bearing as a pulley. A standard SR-4 strain indicator is used for readout of both bridges; the selection is by a four pole double throw switch.

The sealed fluid delivery and discharge pressure is measured by two bourdon gauges which have been calibrated on a dead weight tester. The pressure at the seal is taken as the average of the two readings since the friction drop is approximately the same for the supply and discharge flow paths. The hydraulic fluid supply temperature is monitored by the thermometer in the reservoir and manually controlled by adjusting the cooling water flow. The spindle speed is measured by a strobotach using the timing mark on the seal ring lockplate. The field and armature currents of the drive motor are monitored by the meters on the control panel.

2.5 Design Changes and Proposed Improvements.

In assemblying, checking out and operating the apparatus a number of corrective changes and improvements were made. Furthermore,

there are several design changes that should be made if another apparatus of this type is designed and built.

1. In designing the spindle [2] the 16N thread was used to allow fine adjustment of the bearing preload. It was found that considerable trial and error was required to achieve satisfactory adjustment for continuous operation. The main difficulties arose from the differential thermal expansions which, under certain conditions, tended to increase the preload and resulted in excessive heating of the bearings. To simplify the adjustment and reduce the danger of excessive preloads a flexible member between the bearing and adjustment nut should be provided in the design. The "loose fit" of the bottom bearing cone must also be carefully maintained if full advantages of such flexible preloading arrangement are to be realized.

2. The tie rods [16] were designed for machining from round rods with ends upset and a portion flattened by forging to provide the cleanup for machining. The available forging facilities and skills were overestimated; therefore, the design of the tie rods should be modified to eliminate the troublesome forging operation. It would be preferable to design the tie rods in two pieces, making the strain gauge mounting portions short so that these could be conveniently machined. This, of course, also requires designing a coupling to join the two sections of the tie rods. Alternatively,

tie rods may be machined in one piece eliminating the coupling. In any case the tubular dowels and hole sizes in the bell housing [10] and spindle housing [11] should be checked for adequate clearance to facilitate the assembly of the apparatus. In the existing design, clearances were allowed for rods, but were not sufficient for the strain gauge connecting wires to pass through. Consequently, the test bench had to be tilted or lifted to install the tie rods from underneath.

3. In using the parallelogram geometry with torque strips for seal friction measurement the fact was overlooked that with the mounting ring in the centered position the centering force component produced by the seal friction torque becomes zero. Thus the system can, and under certain conditions does, behave as a self-excited oscillator resulting in severe vibrations. This condition was corrected by designing stops that kept the mounting ring vibrations from building up. These stops consist of small ball bearings which are mounted on two additional posts in the torque ring [25] and are adjustable with respect to the cylindrical side of the mounting ring.

4. The labyrinth seals at the top end of the spindle, as initially designed, were not adequate. Two slinger rings had to be added to the seal adapter [4] and a baffle into the bore of the spill channel [27] . In addition the skirt of the lock ring [26] should be lenghthened about 0.2 inch to reduce the fine spray that occurs at high leakage rates as the oil is slung into the spill channel.

At the bottom end of the spindle, the labyrinth sealing the cooling oil spill groove was adequate with rotation; however, the groove was too shallow to provide sufficient head for drainage by gravity. This was anticipated in the design but could not be corrected easily due to space limitations. The problem was eliminated by adding a small scavenge pump to the bearing supply system.

A third sealing problem was encountered under certain conditions with stationary spindle and high seal leakage rates, e.g. when establishing the zero torque reading. It was found that seal leakage found its way into the spill groove for the bearing cooling oil although there was no spilling over the outer edge of the spill channel which is lower than the inner edge. A pressure differential sufficient to overcome the elevation difference between the inner and the outer lip of the spill channel [27] apparently was created by the suction of the scavenge pump or the syphon effect when the flow rates were such that a liquid seal was formed in both the spill channel [27] and the spill groove of the bell housing [10] . To rectify this condition tangential vent holes were drilled into the lock ring skirt [26] to eliminate the pressure differential.

The experience gained emphasizes three important points in designing labyrinth seals; overlap should be made as big as possible, the secondary leakage due to splash and ricocheting of the fluid thrown from slingers may be significant, and labyrinth seal operation under different fillup levels must be considered in order to ensure

proper venting, particularly if several labyrinth seals are interconnected in some way.

5. During experimental runs several premature seal ring failures were caused by sudden drops in the seal supply pressure. In such cases the test seal had to be relapped and at least part of the test run repeated.

The unexpected pressure drops are caused by the sticking of the accumulator piston. It may be possible to reduce the severity of these sudden pressure drops to some extent by dismantling and cleaning the accumulator; however, the problem still remains because some Coulomb friction will always be present. The pressure variations are relatively severe because the supply pressures used in the experiments are very low (less than 500 psi) compared to the accumulator rating of 3000 psi.

The solution to this problem is a diaphragm type accumulator with a pressure rating that is closely matched to the experimental pressure range. If desirable, the supply pressure variations can be further reduced by connecting an auxiliary compressed air tank to such an accumulator.

6. Based on the friction coefficient values calculated from experimental results, a drive motor of 3 to 4.5 hp is needed to cover the entire range of operation parameters and seal sizes of the apparatus. However, a new motor is not essential until the

experiments with the seal sizes and operating conditions within the capacity of the existing drive motor have been completed. The power rating of the present 1.5 hp motor can be readily extended by at least 30 per cent by providing forced cooling. The forced cooling ducts can be connected directly to the motor vents without any access or space problems.

7. Under certain operating conditions it may be desirable to measure friction torques so low that tensile forces on torque strips are less than 0.5 pound. In that region the stresses in strain gauge backing and bonding materials become relatively more important, and strain gauge bridge response becomes nonlinear and less accurate. The nonlinearity and increased scatter of calibration points can be seen in the calibration curves for torque strips*. The above effects can be suppressed with a bias load applied to the mounting ring. The simplest method would be to use two hanging weights on thin strings fastened to the mounting ring and running over small pulleys mounted symmetrically on the torque ring. This design modification has not been necessary because so far in mechanical seal experiments low torques were encountered only with high leakage rates; an operating region of little interest.

2.6 Summary.

From the full scale design layout, part of which is shown in

---

*Figure 21 in the appendix.

Figure 1, complete detail drawings were prepared for every component of the apparatus. These drawings are up to date with respect to all the design changes and represent the apparatus in its present form. The detailed drawings are too big and numerous to be included in the body of the thesis; however, prints or microfilm copies can be made when needed from the originals that are filed in the Mechanical Engineering Department.

The apparatus design may be considered successful because:

1. The apparatus in its final form satisfies the experimental requirements and design specifications.
2. No major design changes were needed after the final design layout was completed.
3. No serious manufacturing problems were encountered.
4. All components were built according to the detail drawings; whenever parts checked out within specified tolerances they assembled as expected.
5. The minor design changes discussed in the preceding section have been or can be carried out without difficulty.
6. The various adjustments provided for in the design have been adequate.
7. In the experimental work no serious difficulties have been encountered that could be considered due to oversights in the apparatus design.

In particular, test seal geometry can be controlled to at least an order of magnitude higher accuracy than in any commercial seal. Using selective orientation when mounting the seal adapter [4], onto the spindle [2] , and by lapping a taper into the seal ring [9] , the axial runout of the test seal face can be made less than 0.00005 inch (i.e. approximately five light bands) without imposing expensive high precision requirements on machined parts or bearings.

The four essential requirements to be satisfied by the basic apparatus configuration proved highly useful in conducting the experimental work. The rather stringent decision to keep all space on one side of the window free of all structure has facilitated the photographic work. It can be seen from the overall view of the experimental setup in Figure 4, that the space requirements for the camera and lights have not been overestimated.

With controlled and measurable axial force capacity up to 8400 pounds the apparatus can also be used for investigating the oil film behavior in thrust bearings of both static and dynamic type. The adaptation for thrust bearing work requires only replacement of the seal ring [9] by a thrust bearing ring; alternatively, a completely new adapter with an integral thrust bearing may be designed. No changes are needed in the glass window or the existing instrumentation.

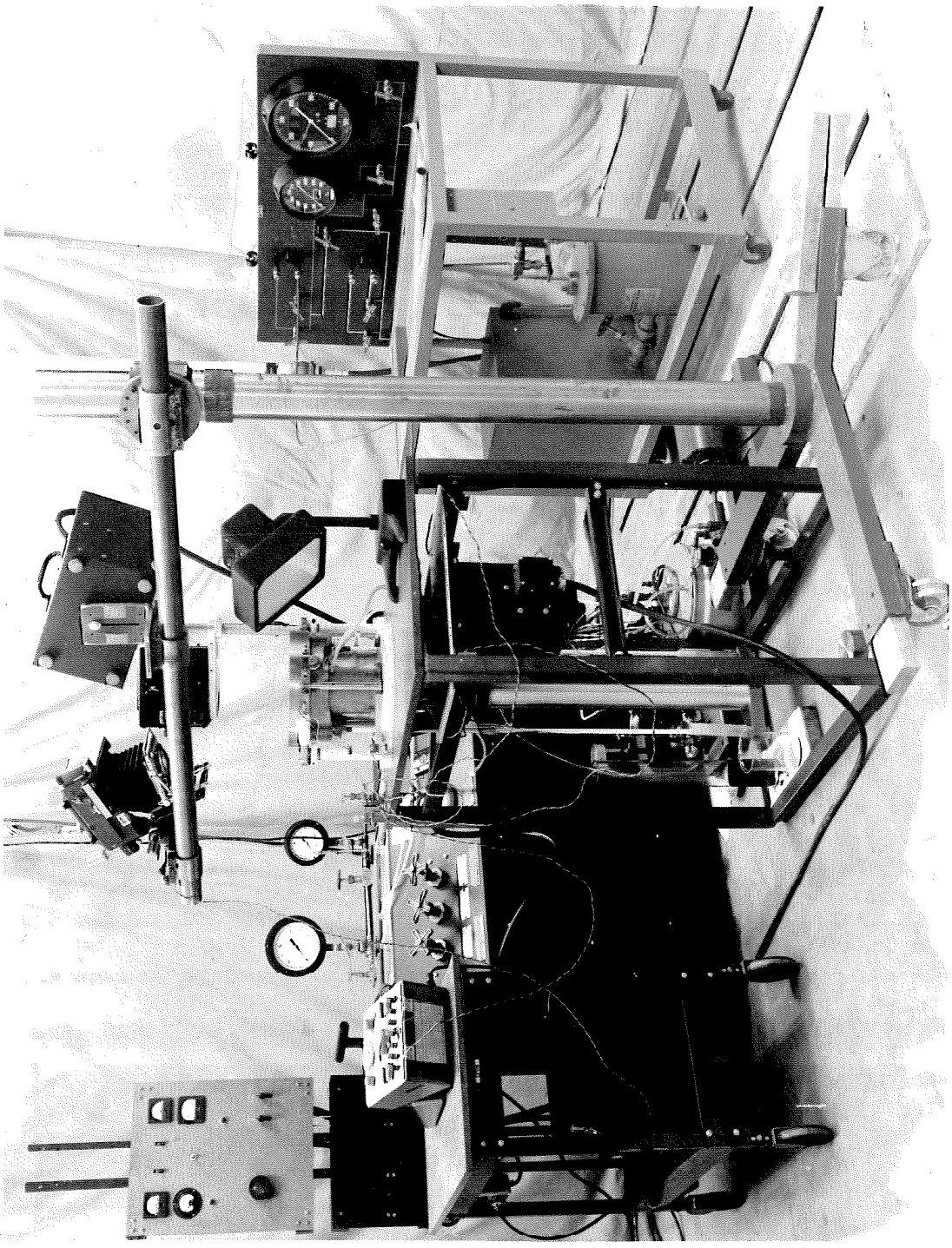

Figure 4. Overall view of the experimental setup.

III. EXPERIMENTAL RESULTS

3.1 Seal Preparation and Clearance Geometry.

The seal faces are finished on cast iron lapping plates charged with diamond powder. To charge a lapping plate, fine diamond powder in paste form is rolled into the plate surface with a hard roller. A roughing and a finishing plate are used, charged with 750 and 1600 mesh powder respectively. The lapped seal faces are checked for flatness with an optical flat under monochromatic light from a helium filled neon tube. All these pieces of equipment are commercially available items.

The seal rings used in the experimental work were machined out of carbon impregnated with babbit which is one of the common materials used in commercial seals. The faces were finished by hand lapping to flatness of one to two light bands over the diameter, or about half a light band per inch. One light band corresponds to the path difference of one wavelength, i.e. a clearance variation of one half the wavelength between the reflecting surfaces of the seal face and the optical flat. With helium light of 5875.6 $\mathring{A}$ wavelength* the unit (i.e. one light band) for measuring the seal clearance variations comes out to be 11.6×10^{-6} inches. Thus in the experimental seals the faces as finished by lapping had curvatures less than 6×10^{-6}

---

*Persistent band with longest wavelength in He spectrum.

inches per inch. The typical fringe pattern of a seal face after lapping is shown in Figure 5a.

The windows cut from plate glass, when checked out with an optical flat, had at least one face of comparable flatness and did not require any lapping.

After carefully lapping and installing the first seal, a check with the optical flat showed that the installed seal ring was not flat. The surface was a concave polar symmetric shape indicated by circular and very closely spaced light bands; the fringe pattern on the seal face was somewhat similar to the grooves in a phonograph record. When the lock plate [8] screws were loosened, the seal face returned to its initial flatness. The first conclusion was that either the back face of the seal or the seal adapter [4] seat were not flat, although considerable care had been taken in their machining. To ensure flatness the back side of the seal ring was lapped to the same flatness as the face, Figure 5b. A special lap with a hole in the center was prepared, checked with the optical flat and then used to lap the adapter seat. The bottom face of the lock plate was also lapped flat.

The seal face in the installed condition after the above changes still showed a concave distortion but to a lesser degree; the fringe spacing was larger, indicating slightly less distortion. A typical fringe pattern on the installed carbon seal ring face is shown in Figure 5c. Estimated face curvature is about 4 light bands

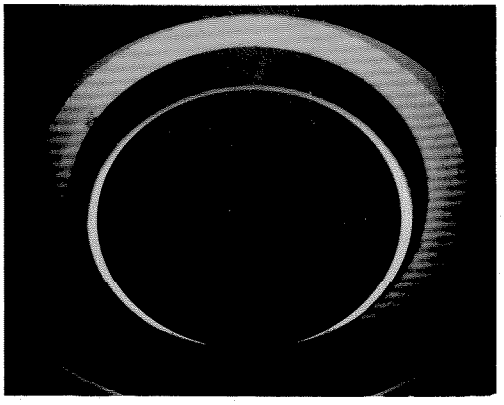

a. Typical lapped face, free, with optical flat.

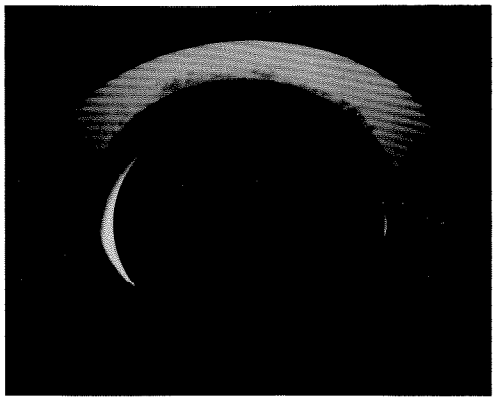

b. Lapped back side, free, with optical flat.

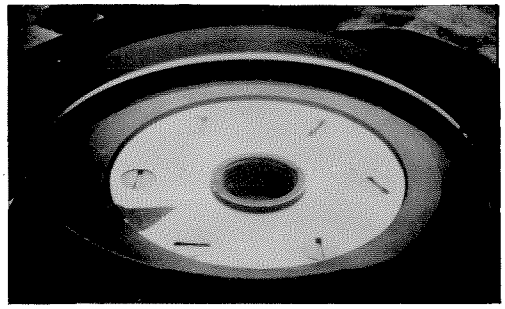

c. Installed, tight on O-ring, with optical flat.

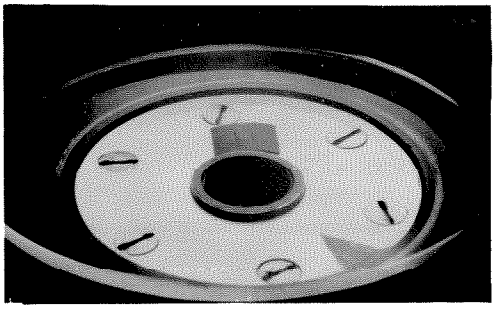

d. After initial failure, tight on O-ring, with optical flat.

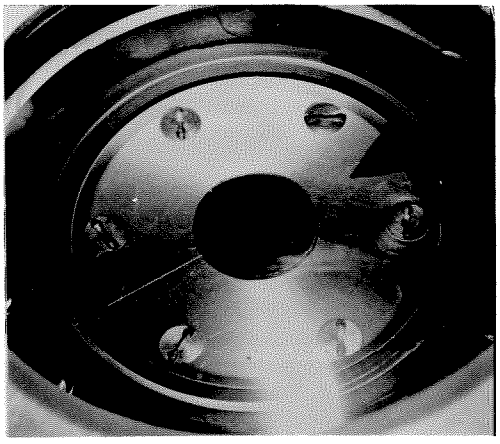

e. Typical initial failure, high speed photograph at 1600 rpm.

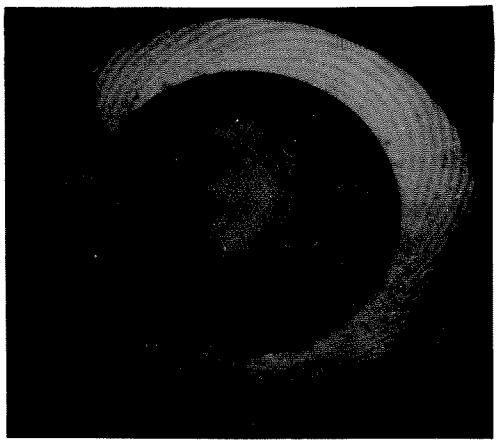

f. Typical permanent set, back side, free, after scoring of the face.

Figure 5.

Distortion and failures of carbon seal ring. 4 in. O. D. - 3. 25 in. I. D.

per inch. The distortion results from the forces needed to compress the O-ring under the seal.

A similar fringe pattern was found with a brass seal ring except the face distortion was about two light bands per inch as may be expected since the elastic modulus of brass is two to four times higher than that of the seal carbon, Figures 6a and 6b. Thus the elastic distortions due to installation stresses can be reduced but not eliminated even by the most careful finishing of the structural parts. It should be pointed out that, in the available literature, only two statements were found (10), (11) emphasizing the importance of avoiding distortions in the supporting structure, e.g. in the seats for the seal rings.

Since in commercial seals the back sides of the seal rings and the supporting surfaces are not finished by lapping, it is obvious that considerably larger distortions must exist and, in some cases, there is also no polar symmetry of the seal face after installation.

If the low installation stresses cause seal face distortions that are excessive according to currently accepted flatness standards, then, under operating conditions with high fluid pressures and big closure forces, much larger distortions must take place. Consequently any assumptions about seal faces being flat are unjustified.

In view of the above experimental evidence it would be of considerable interest if the shape of the seal faces, i.e. the

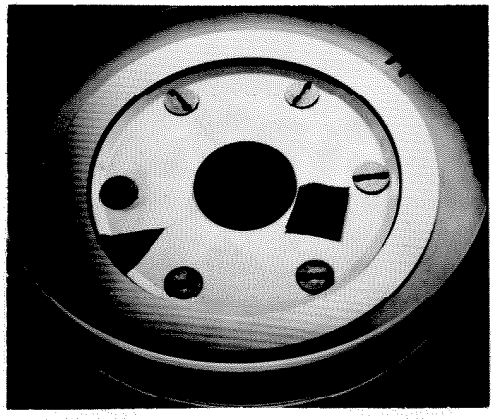

a. Seated, free, with optical flat.

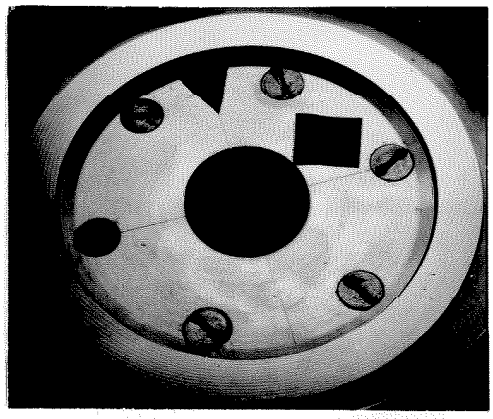

b. Installed, tight on O-ring, with optical flat.

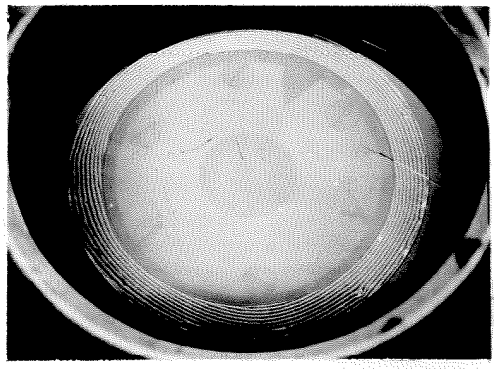

c. As installed with plate glass, average seal face pressure 9.4 psi.

d. As installed with plate glass, average seal face pressure 321 psi.

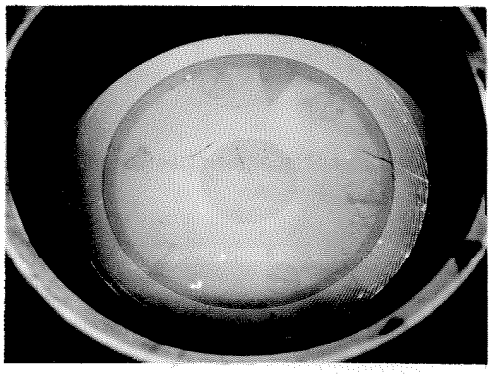

e. Stationary with 130.4 psig oil pressure. Average seal face pressure 68.7 psi.

f. Rotating at 1000 RPM with 130.4 psig oil pressure. Score line in the middle of face.

Figure 6.

Distortion in brass-glass seal 4 in. O.D. - 3.25 in I.D.

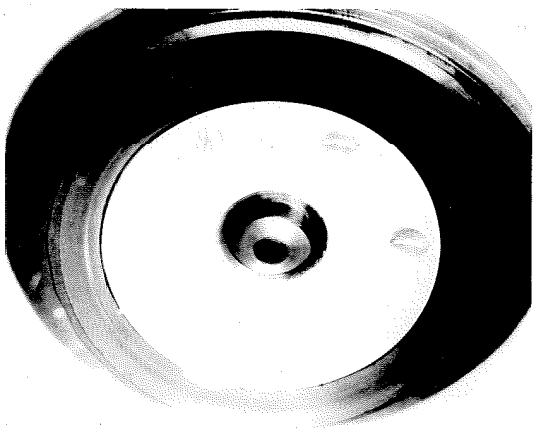

a. Infrared photograph of incipient seal failure, taken immediately after stopping with Wratten No. 25 filter, 1/25 sec at f = 4.7.

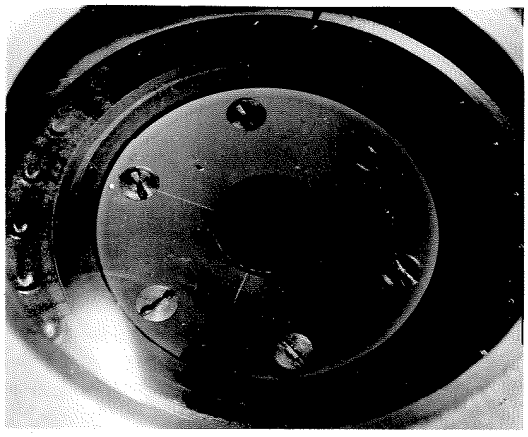

b. Incipient failure with three unsymmetrically located high spots. High speed Microflash photograph at 1800 rpm and f = 8.

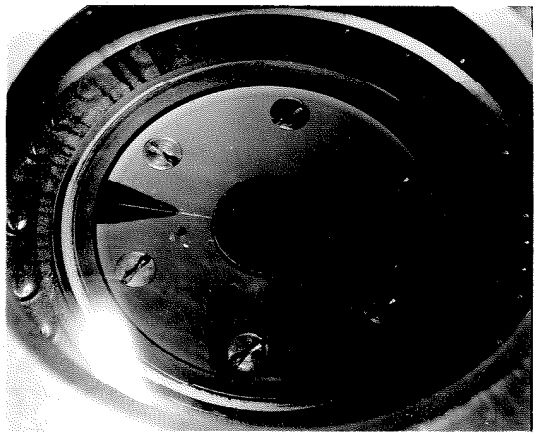

c. Typical failure at intermediate stage. High speed Microflash photograph at 1800 rpm and f = 8.

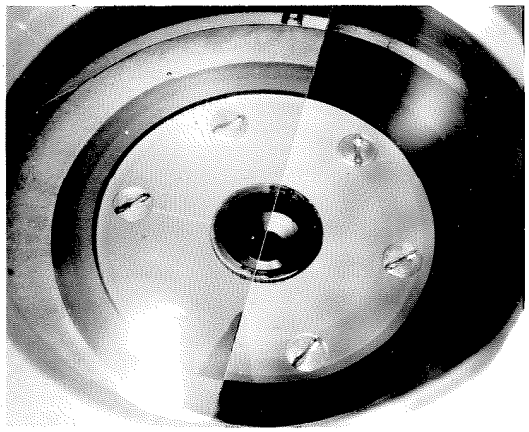

d. Attempt to detect thermal gradients in the seal face. Microflash photographs at 1000 rpm, P = 130.4 psig, β = 0.79.

Left half--ordinary film at f = 8.
Right half--infrared film with Wratten No. 25 filter at f = 4.7.

Figure 7.

Ordinary and infrared photographs of carbon-glass experimental seal.

clearance geometry, in an operating seal could be measured, or at least deduced. Direct measurements were out of the question because of the access problems to the operating seal faces. Measurement of overall strains, such as changes in the position of the stationary window, were investigated, but such effects either did not occur or were too small to be detected by conventional dial indicators which can resolve 0.0001 inch. The ordinary interferometric techniques, similar to the one used for checking flatness of lapped seal faces, do not work in the presence of the oil, because the refractive indices of glass and oil are not sufficiently different to result in partial reflection at the glass-oil interface in order to produce observable fringes. The carbon face seal, even when highly polished, is a very poor reflector which makes any interference fringes difficult to see and to photograph. The monochromatic light used for seal face inspection is of rather low intensity requiring time exposures which make photography of changing fringe patterns impossible. Other light sources were considered and the most suitable one for this work appears to be a gas laser; it has excellent monochromaticity and high intensity. Unfortunately, an available laser could not be found for the first series of tests.

A seal ring made of brass was tried to improve reflectivity of the seal face. This produced fringe patterns of slightly better contrast and permitted reduction of the exposure time for photography by at least an order of magnitude. The typical fringe patterns with

a brass seal and an optical flat are shown in Figures 6a and 6b. However, this combination still did not produce fringes with oil in the seal clearance. The problem was resolved by experimenting with vacuum deposited metal films to form a half-mirror on the glass seal face. A half-mirror formed by chromium film turned out to be best, because of reasonable abrasion resistance, although it was optically poorer than an aluminum half-mirror. Some metallic salts have good semi-reflector properties, however these were not tried because there were no facilities available for depositing such films; also their abrasion resistance was not known*.

The chromium film half-mirror in combination with a brass seal produced fringe patterns of good contrast with oil present, even under running conditions. Typical fringe patterns are shown in Figures 6c, 6d, 6e and 6f. Unfortunately, a brass-glass seal is very delicate and easily damaged because glass has lower tensile strength than brass. Surface tractions caused by dry rubbing contact produce tensile failures in the glass commonly known in the glass trade as chatter sleeks. Since refinishing of the glass surface requires special facilities and is relatively expensive, the test runs with brass-glass seals require great care to avoid damage to the half-mirror before observation or photography can be carried

---

*A film of zinc sulphide produces an excellent semi-reflector for interferometric work, it has a high index of refraction compared to glass, and almost no absorption[12].

out. Operation with boundary lubrication over the entire seal face is impossible because damage occurs before this condition can be approached.

With carbon seal rings the fringe patterns are too faint to be seen; however, the shape of the rotating face can be deduced from the high speed photographs of the seal face failure. For these photographs high intensity flashes from a General Radio Company Microflash were used to stop the motion. Typical seal face failures are shown in Figures 5e and 7b, 7c. Wear patterns at different stages of failure were also photographed under stationary conditions, Figures 5d and 7a.

Infrared photography was tried to detect thermal gradients in the carbon seal face, Figures 7a and 7d. These attempts were unsuccessful, probably because temperatures at the experimental seal face were so low that the wavelength of the emitted infrared radiation fell outside the transmission limits of the plate glass window.

3.2 Observation of Fluid Film.

One of the controversial questions of mechanical seal design is behavior of the fluid film in the seal clearance. Several theories have been proposed; however, these all hinge on some assumed simple form of the fluid film in the clearance space. Some pressure distribution measurements across seal faces have been carried out[4] but meaningful interpretation of the results is difficult or impossible for the following reasons. Seal clearances are so small that

any pressure tap or other sensing device is at least an order of magnitude bigger than the film thickness, and its presence changes the conditions in the film. In such case, cause and effect cannot be separated and the data become unreliable. Pressure distribution measurements are meaningful only if the fluid film in the clearance is continuous at the point of measurement.

Two of the doubts to be resolved by visual observation were the extent of the continuous fluid film, and its dependence on the other operating variables.

During the first few test runs it was found that, after starting with a continuous film over the entire seal face (i.e. substantial leakage), gradual increase of the closure force produced a progressive breakdown of the continuous film. The transition from full film to boundary lubrication started at the outer periphery and spread inward over the entire seal face. Further increase of the closure force eventually resulted in failure by scoring of the carbon seal face. Since incipient failure could be observed, the apparatus could be stopped at any stage of the failure.

With proper oblique illumination, fine striations with silvery reflections could be observed and the transition line between the continuous and discontinuous film could be distinguished. Unfortunately, due to extreme thinness of the film, the contrast was very poor and, although the phenomena is polar symmetric, it could be

observed only over a small angular portion at a time. When there was boundary lubrication over the entire seal face no striations could be observed since the transition line between the full film and the boundary lubrication region disappeared. There was, however, no ambiguity when the boundary lubrication condition over the entire seal face was reached because this always brought about torque fluctuations indicating a stick-slip condition.

Several light sources were tried to improve the contrast, but an ordinary hand-held floodlight, that could be moved around to vary the incidence angle, proved to be the most useful. No satisfactory photographs could be obtained and it was necessary to rely on records of visual observations throughout the tests for correlation with other measured experimental data.

The light sources that were tried without success include a standard strobotach, an ultraviolet lamp and single high intensity flashes of short duration from a General Radio Company Microflash. A new type strobelight producing repeated flashes of higher intensity than the strobotach may be useful but such an instrument was not available at the time of the tests.

3.3 Numerical Data.

The variables measured in the seal tests are supply and discharge pressures of the sealed fluid*, axial closure force, seal

---

*Hydraulic oil was used in all tests, the temp.-viscosity curve is given in Figure 18.

friction torque, rotational speed and leakage. The readings were taken at regularly timed intervals, except for the leakage which was measured for the entire interval at each experimental setting. The above measurements were used to calculate the reduced data. In addition to these measurements the hydraulic pressure in the load cylinder, drive motor current and seal supply reservoir temperature were monitored to maintain steady state operation and to provide a consistency check on the other readings.

To get reasonable accuracy in the numerical data, particularly with low leakage rates, the measurements had to be taken over a sufficiently long time interval with steady state conditions maintained as closely as possible. After initial warmup of about one hour, at least a 15 minute interval was needed to achieve a reasonably steady state for each new test setting. When the steady state was reached, readings were taken at 3 minute intervals over a 15 minute period. At settings with high leakage rates (over 1 cm^3 per minute) periods as short as 9 minutes were used.

Readout of the numerical data, recording of the data, and monitoring of the equipment during the tests was done visually. A single strain gauge indicator was used for both the closure force and the friction torque measurement. For these reasons, with one man operation, the different readings were taken sequentially although they are recorded as simultaneous. To take a set of

readings required from 30 to 60 seconds and the exact time was observed only in the leakage measurement. The torque readings varied by the largest amount; these were taken before measuring the closure force and checked again afterwards.

The operating parameters for the test seals were calculated as follows:

1. Sealed fluid pressure $P = \frac{1}{2}(P_S + P_D)$ -[psig], where P_S and P_D readings are corrected by the calibration curves for the pressure gauges; Figure 19.

2. Total closure force $F = C_1 r_F + w$ -[lb], where the constant C_1 is determined from the calibration curve in Figure 20.

3. Net force on the seal face $N = F - P\frac{\pi d^2}{4}$ -[lb]

4. Average seal face pressure $\bar{p} = \frac{N}{A}$ -[psi]

5. Shear force at the average seal face radius $S = \frac{10.5}{\bar{D}} C_2 r_T$ -[lb], where C_2 is a constant or a value determined from the appropriate calibration curve; Figure 21.

6. Average shear stress $\bar{s} = \frac{S}{A}$ -[lb/in^2]

7. Friction coefficient $\mu = \frac{S}{N} = \frac{\bar{s}}{\bar{p}}$

8. Balance ratio $\beta = \frac{\bar{p}}{P}$

As already mentioned, the technical literature on mechanical seals abounds in design descriptions but numerical design data either does not exist or is considered to be proprietary information and is

therefore not available. The goal in all designs is to eliminate the leakage, or at least to reduce it to a tolerable level. It has been generally accepted that the ordinary laminar flow equation (based on the assumption of a parabolic velocity profile in the uniform clearance)

$$Q = \frac{\pi \bar{D} z^3 P}{12 \eta b} \times 39.3 \quad - \left[\mathrm{cm}^3/\mathrm{min}\right] \qquad (1)$$

does not give correct leakage rates. Consequently, either the flow is not laminar or the applicable η and z values are not known. The importance of adequate cooling for good seal performance is repeatedly emphasized; however, friction data to estimate cooling needs is again notably lacking.

Useful parameters for designing mechanical seals and predicting their performance cannot be found in the current literature. One of the goals in these initial tests was to establish the parameters relating seal performance to the operating variables. More systematic testing could then be undertaken to evaluate these parameters more closely.

Reduced data from about a first dozen test runs showed no correlation or trend when leakage rate Q was plotted against speed of rotation n, sealed pressure P, or seal face pressure $\bar{p}$. Similarly, the friction coefficient μ was found to be not dependent on any single factor.

In these initial test runs the supply reservoir temperature was not controlled and a temperature rise of 10° to 30° F took place over the duration of a test run. This can change the viscosity of the sealed fluid at most by a factor of two. However, even allowing for viscosity variations, the wide scatter of experimental points could not be explained*.

Using the pressure-velocity factor** $P\bar{v}$, as the independent variable no correlation could be found.

When leakage, Q, was plotted against the balance ratio, β, a trend could be detected, particularly if allowance was made for the slow temperature rise of the sealed fluid during each test run.

In the next set of test runs a longer warmup period was allowed to reduce the sealed fluid temperature rise during a test run. Supply and discharge pressures were closely monitored to maintain a constant pressure P at the seal within the reading accuracy of the gauges (about $\pm$ 0.5 psi). The additional data indicated a definite trend on graphs of leakage rate Q versus balance ratio β. There also appeared to be some influence of supply temperature t and speed of rotation n.

---

*For unbalanced seals absolute viscosity η is claimed to have no influence on leakage (4).

**$P\bar{v}$ factor-psi×fpm is used by some manufacturers as a limiting parameter in seal applications.

At this stage a cooling coil was installed into the seal supply reservoir and all subsequent test runs were made with at least one hour warmup period. Constant seal supply temperature, pressure and speed were maintained throughout each test run. The closure force was increased in small steps until seal failure took place. The seal was then relapped for the next test run.

The reduced data from test runs No. 20 to 39 is presented graphically in Figures 8 to 17 together with the pertinent values of the seal operation variables. Two empirical relations have been established between the test seal leakage rate, Q, and the friction coefficient, μ , and the seal balance ratio, β.

The experimental points on Q versus β graphs in Figures 8 to 12 represent composite values of several readings for each experimental setting. Different symbols are used to distinguish points from different test runs and the scatter of the calculated values at each point is indicated by the length of the horizontal line through the respective point.

On μ versus β graphs in Figures 13 to 17 all experimental points are shown using different symbols to distinguish data from different runs. The lines are drawn as best approximations of the friction coefficient values up to the highest β-value before failure of the test seal took place.

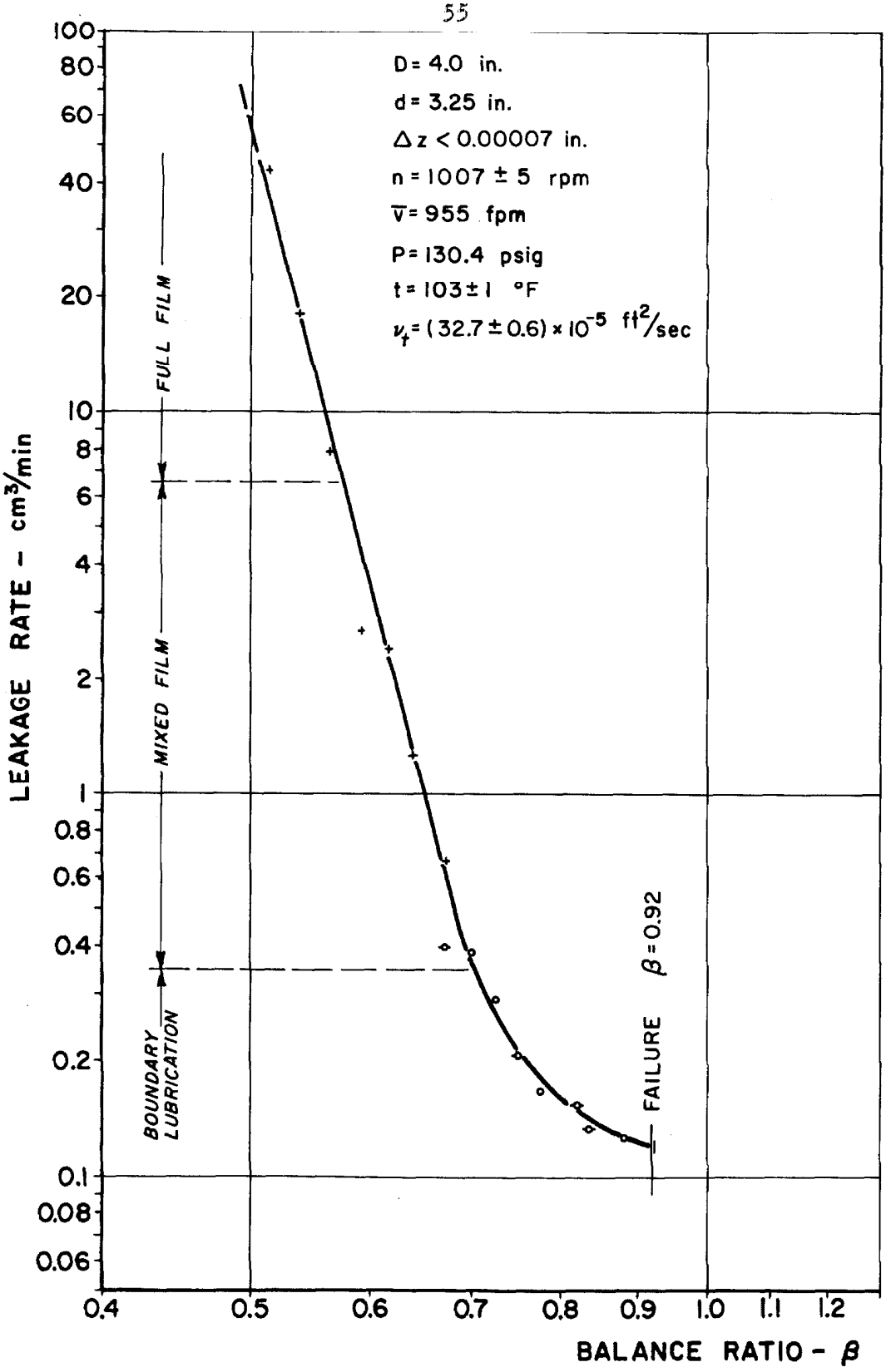

Figure 8. Leakage rate vs. balance ratio. Glass-carbon seal.

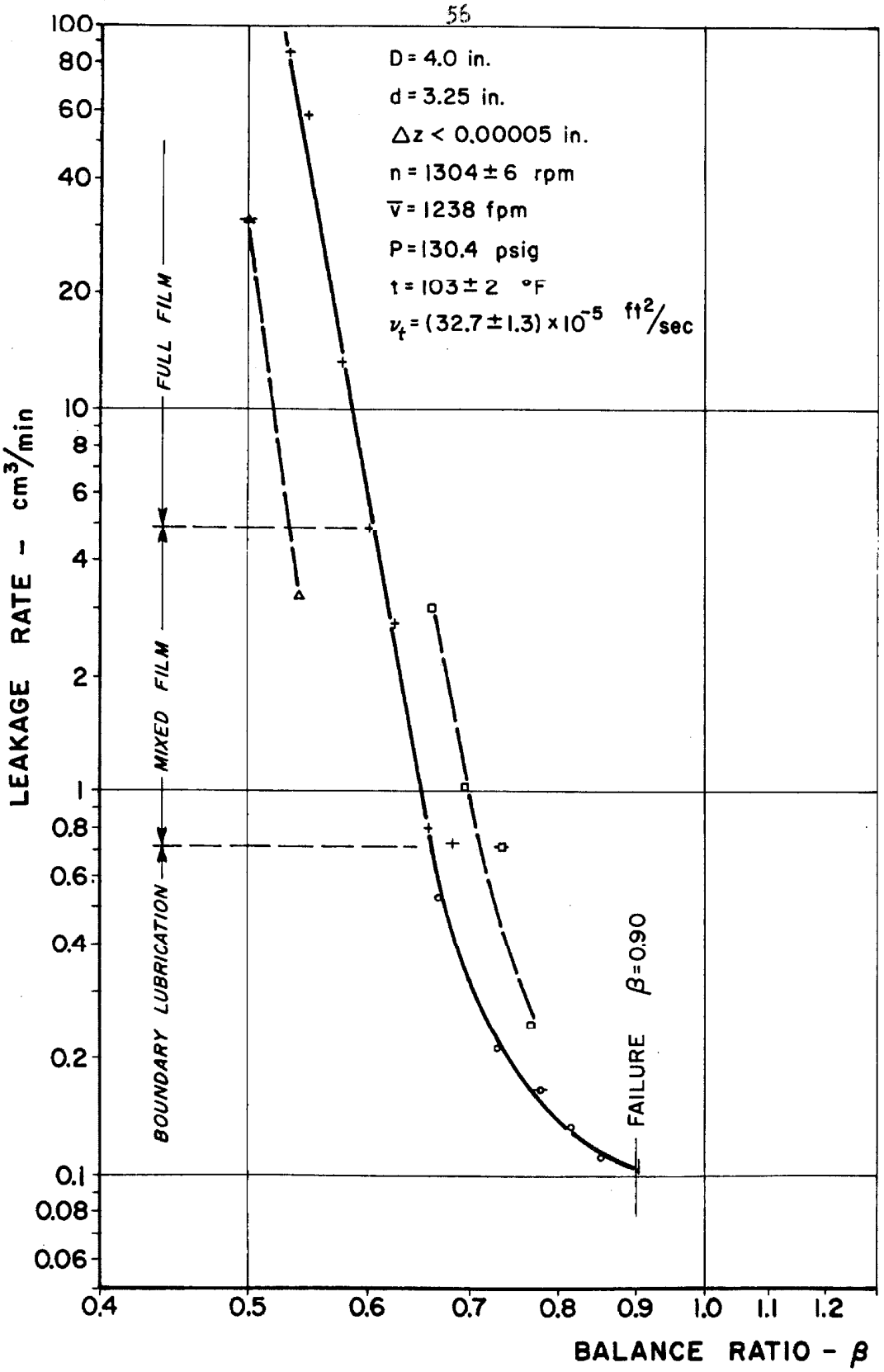

Figure 9. Leakage rate vs. balance ratio. Glass-carbon seal.

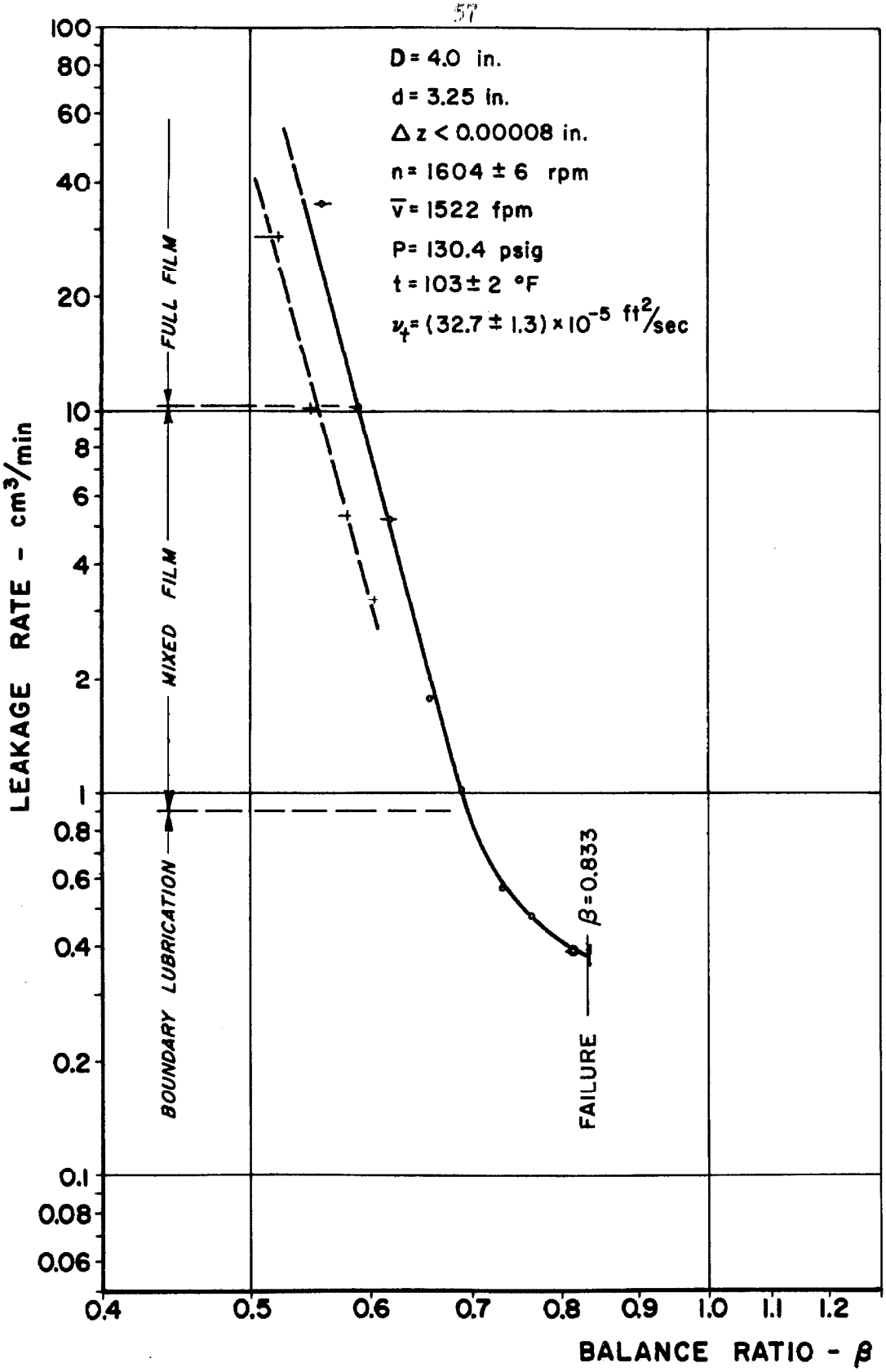

Figure 10. Leakage rate vs. balance ratio. Glass-carbon seal.

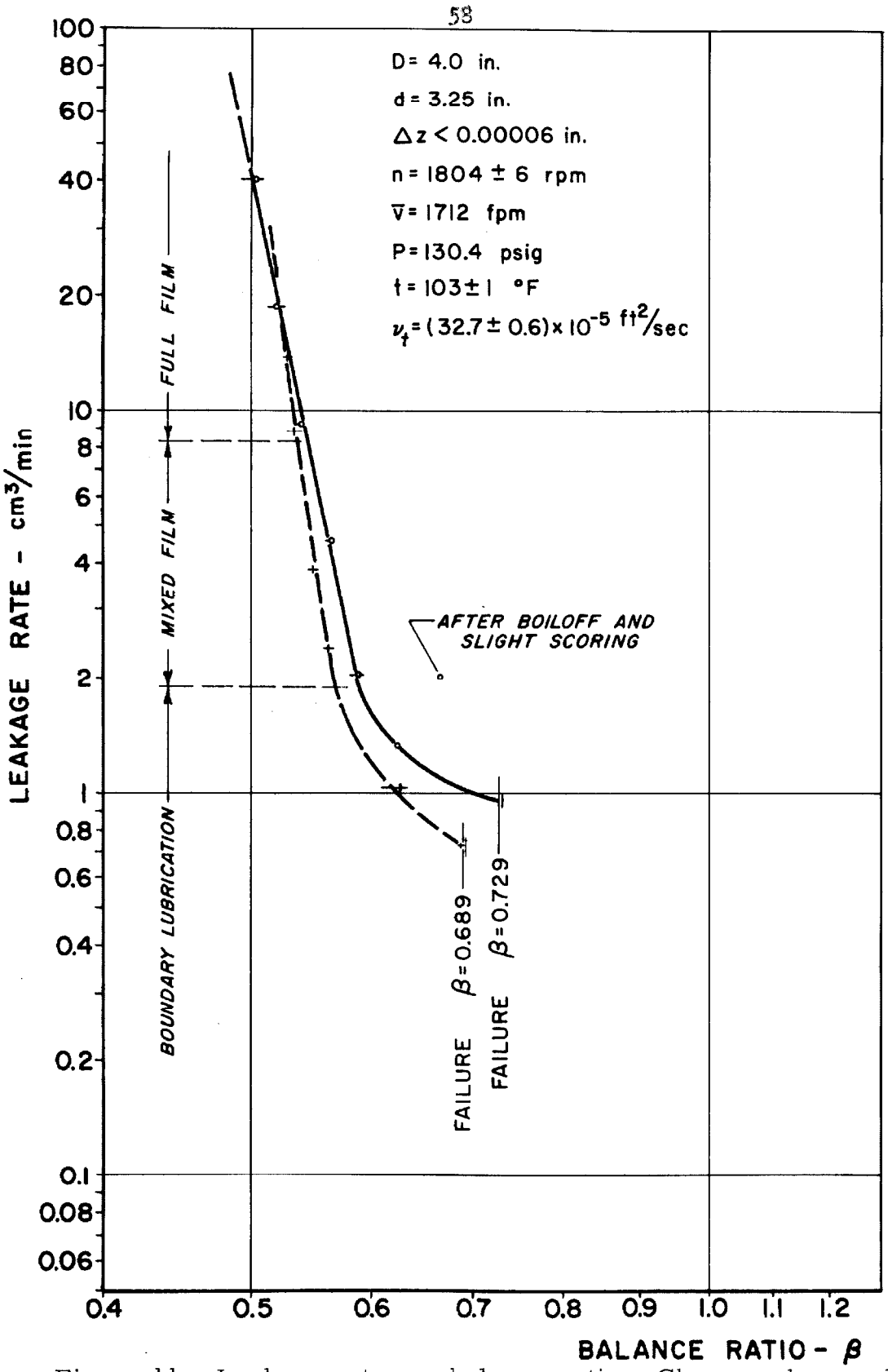

Figure 11. Leakage rate vs. balance ratio. Glass-carbon seal.

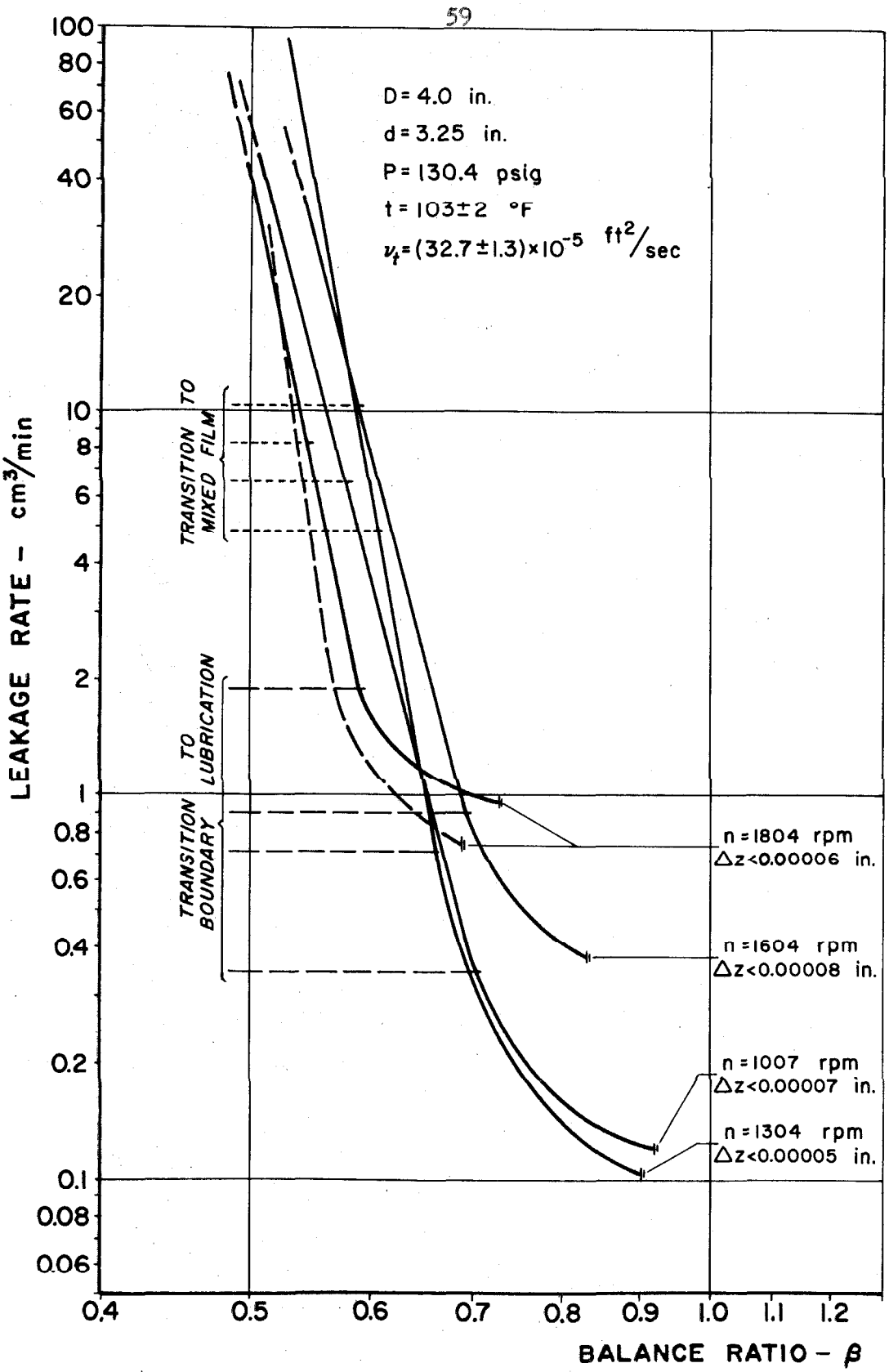

Figure 12. Comparison of leakage rate vs. balance ratio curves.

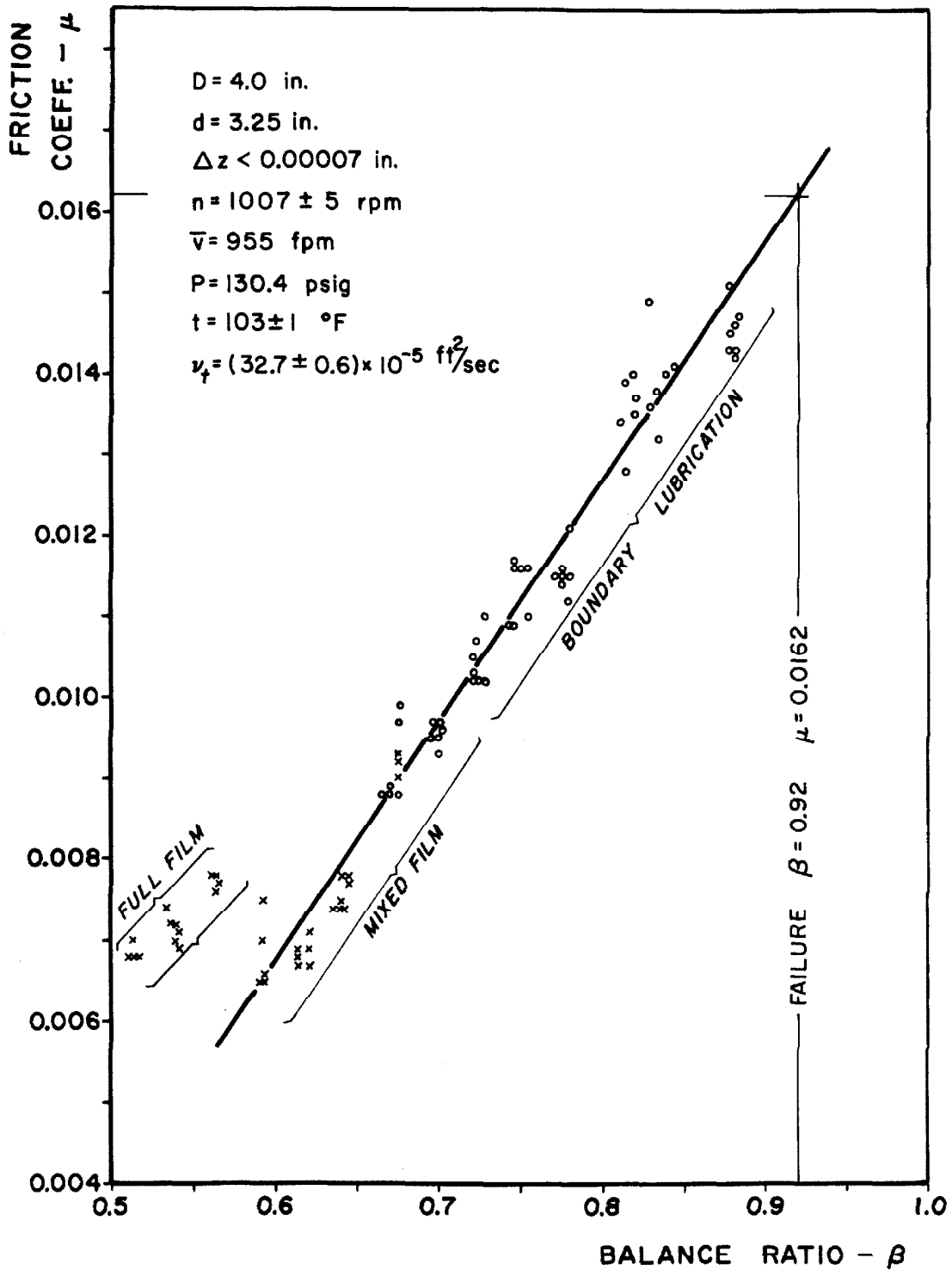

Figure 13. Friction coefficient μ vs. balance ratio β
Glass-carbon seal.

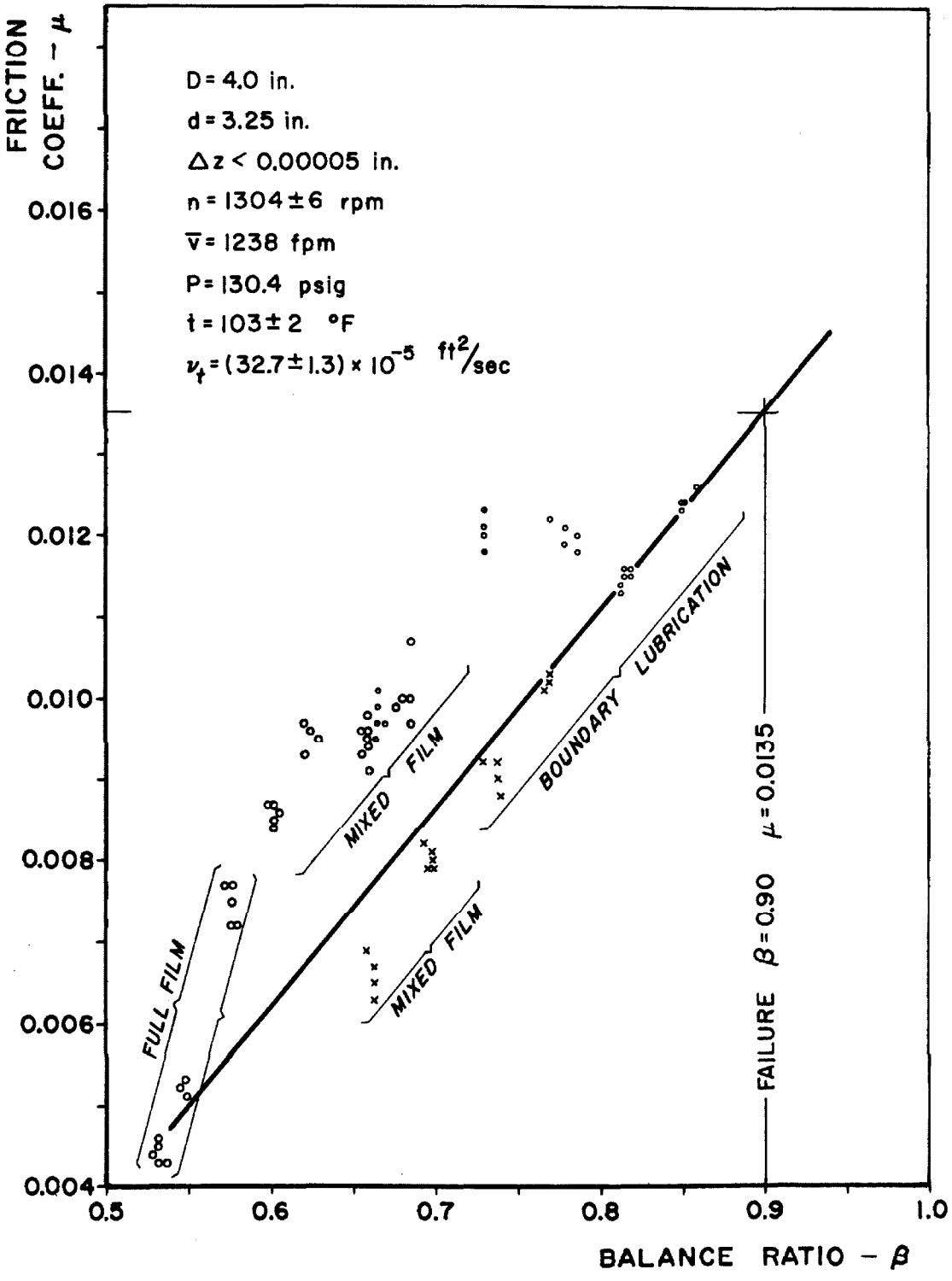

Figure 14. Friction coefficient μ vs. balance ratio β. Glass-carbon seal.

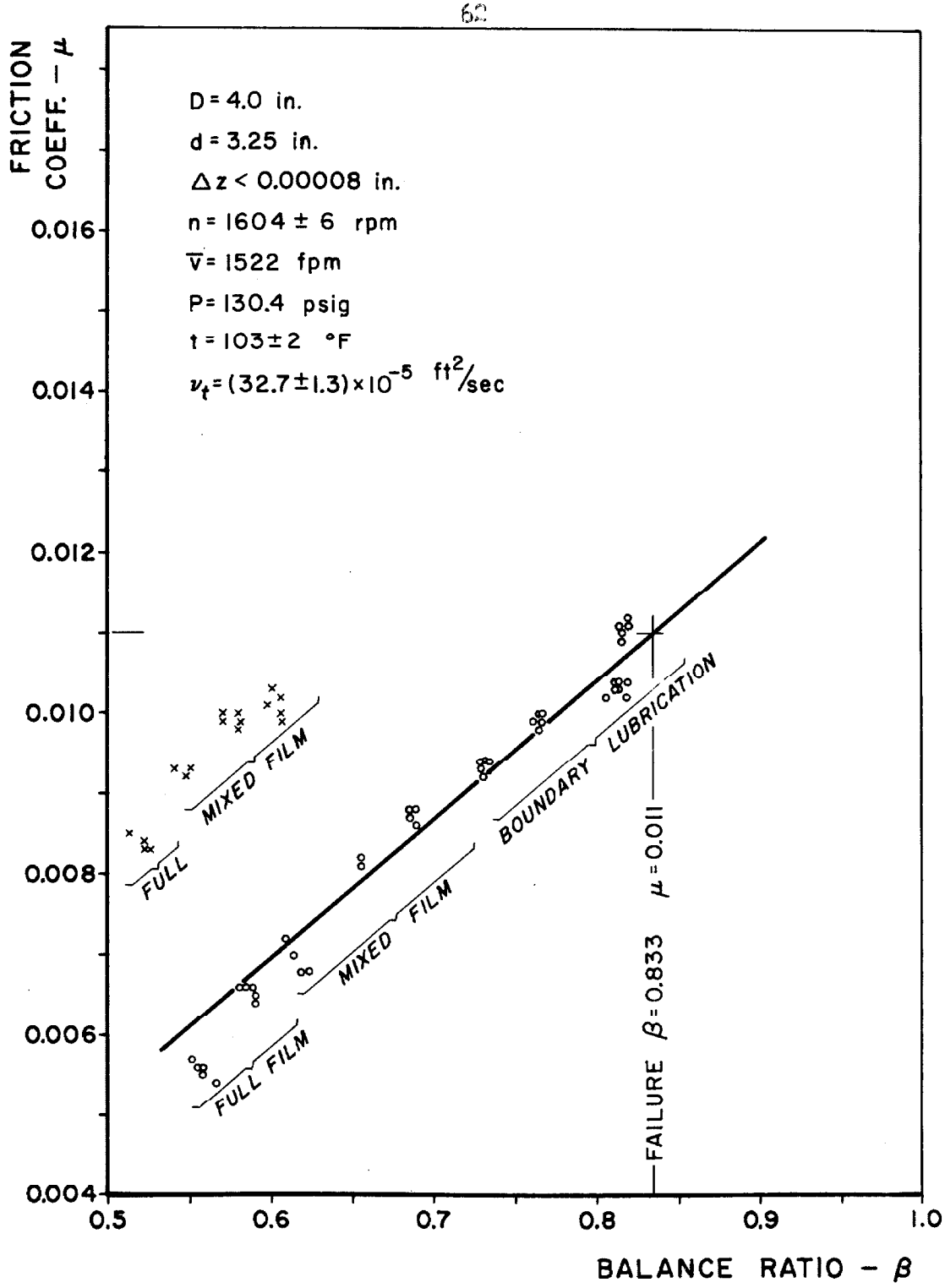

Figure 15. Friction coefficient μ vs. balance ratio β. Glass-carbon seal.

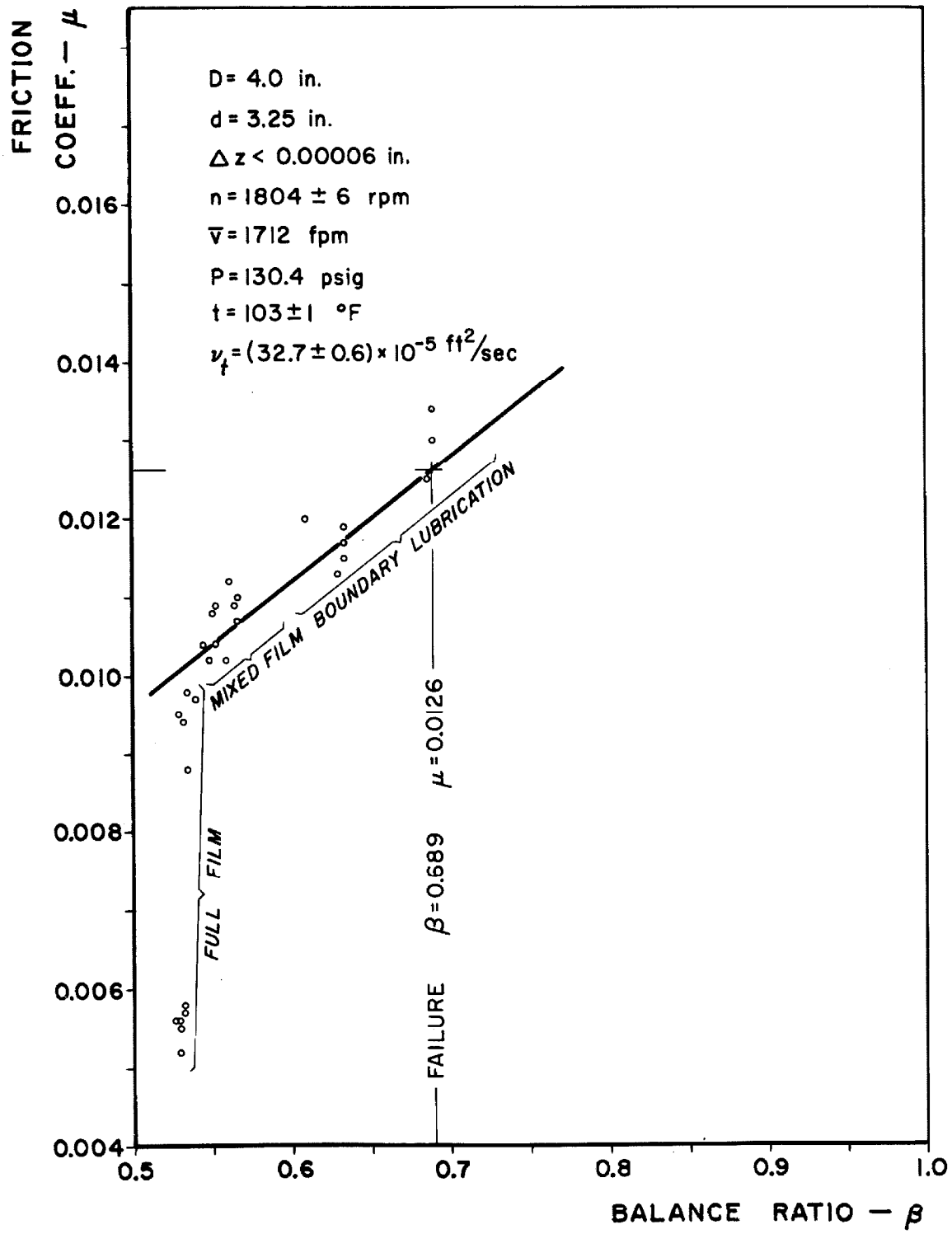

Figure 16. Friction coefficient μ vs. balance ratio β. Glass-carbon seal.

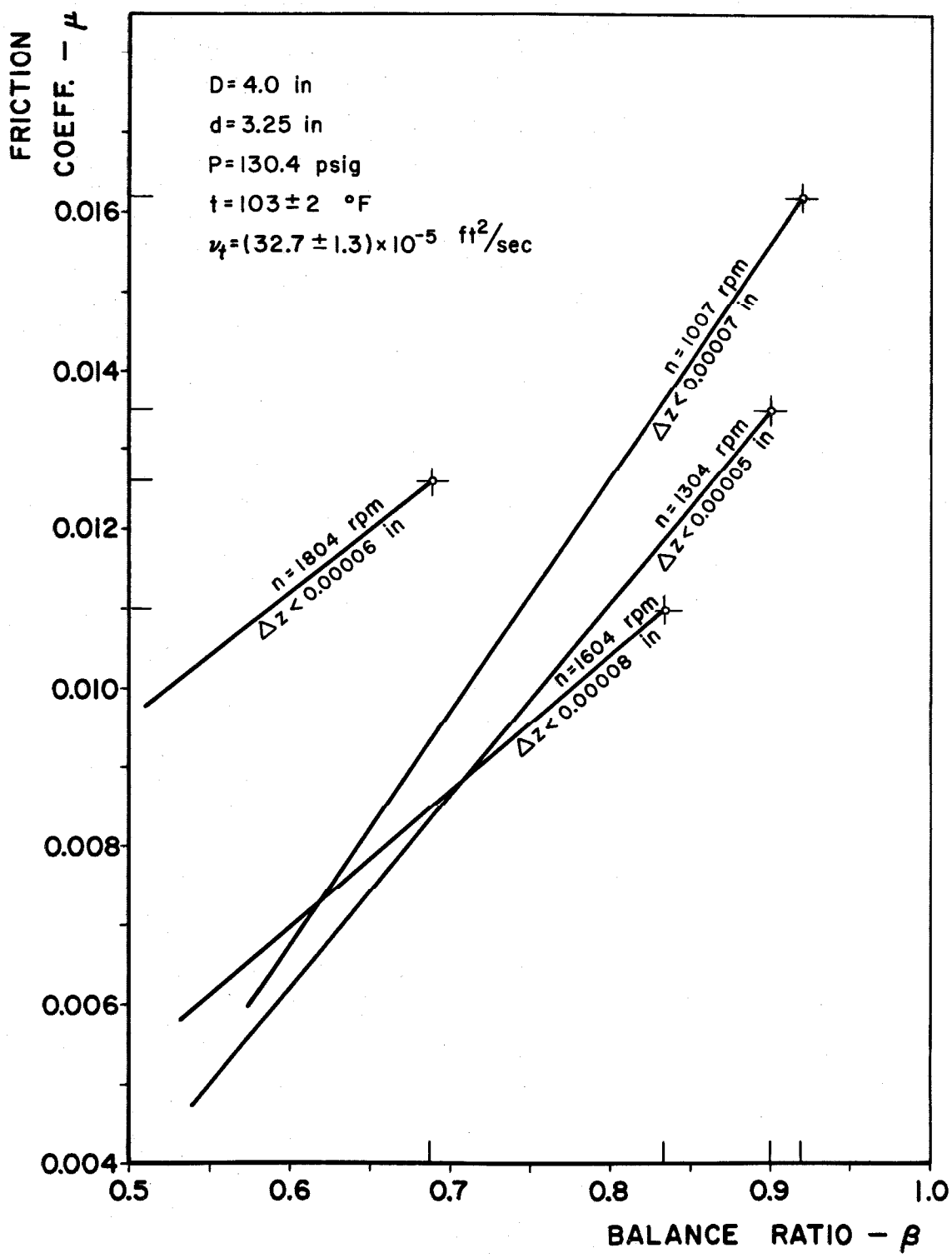

Figure 17. Comparison of friction coefficient μ vs. balance ratio β curves for different speeds. Glass-carbon seal.

3.4 Discussion of Experimental Results.

The interference fringe patterns between a seal ring and the window disc or optical flat show that the clearance, z, between two seal faces under stationary conditions is not uniform. The amount of clearance variation and the direction of the taper depends on the installation stresses and pressure forces from the sealed fluid, i.e. on the design of the structural parts and the secondary seals between these parts and the seal rings. If seal rings are lapped on both sides and supporting surfaces are carefully finished it is possible to keep the elastic distortions of the carbon seal ring polar symmetric. However, the clearance is still not polar symmetric unless the mating seal face is also similarly supported; this is a practical impossibility. Even with a structurally stiff mounting ring and a thick window seated on a flexible gasket the closure forces produced a bending distortion of the glass resulting in the total gap variation of the order of 50×10^{-6} inches, Figures 6c, 6d. As already discussed, in commercial seals only the seal faces are lapped and therefore it is reasonably certain that when installed both seal faces are neither flat, nor polar symmetric within the initial finishing accuracy.

Sealing Mechanism in a Stationary Seal. With a stationary seal, zero leakage condition can be achieved only if the net pressure between faces, $\bar{p}$, is sufficient to overcome face distortions to the

extent that at least a solid-to-solid line contact is produced around the seal face. With liquids, it may only be necessary to reduce the maximum clearance to such low level that surface tension forces exceed the pressure differential. For these reasons the reduction of installation distortions becomes increasingly important for seals that must seal high pressures under both stationary and rotating conditions.

Sealing Mechanism in a Rotating Seal. Under rotating conditions the seal face geometry changes due to the thermal gradients in the seal ring that are built up in order to conduct away the heat generated by the shear between the faces. These thermal distortions take considerable time to develop and to reach a steady state, provided that operating conditions remain reasonably stable. The transient conditions leading to the stable state are of considerable importance if the seal is to reach stable operation without damage. The seal failure by excessive local heat generation will be discussed later with the numerical data. At this stage suffice it to say that during the transient conditions leading to a stable operation, the amount of frictional heat generated per unit area must not exceed the failure value for the particular seal at any time. For the purposes of discussion of the sealing mechanism, three different operating regimes will be considered although, in actual operation, there is no distinct dividing line separating one operating regime from another.

1. Continuous or full film extending over entire seal face. The seal operates as a thrust bearing, with considerable leakage; the axial load is supported by the fluid pressure between faces. The fluid pressure is partially due to the radial flow pressure gradient and partially to the circumferential hydrodynamic pressure gradients in the nonuniform clearance of the seal produced by elastic distortions. The shear rates in the fluid film are relatively low, little heat is generated, and stable conditions are maintained as long as leakage is sufficient to carry away the heat. There is little thermal distortion because most of the heat is carried away by the leakage. This operating regime is at the lowest possible balance ratios without opening up the seal faces, i.e. balance ratio β from 0.5 up to about 0.6 depending on the rubbing velocity $\bar{v}$.

2. Mixed film operation. Under this condition continuous fluid film extends over part of the seal face; over the remaining portion the fluid film is broken up and occasional rubbing with boundary lubrication takes place. The axial force to separate the seal faces is generated primarily by the circumferential wedges formed by the elastic and thermal distortions of the seal ring. The clearance, z, is so small that variations in gap of less than 0.0001 inches result in sufficient taper to convert a seal ring into an effective thrust bearing. For example, the brass-glass seal in Figure 6e at 1000 rpm shows a circumferential clearance variation due to glass distortion alone of eight light bands or about 0.00009

inch. The additional variation from seal ring distortion cannot be estimated from the photograph because the exposure time is too long to stop the motion of the rotating member. With the mixed film the balance ratio, β, is higher; in the experimental seal it varied from 0.6 to about 0.7. The leakage rate is greatly reduced and most of the friction heat must be conducted away through the seal rings and the supporting parts; therefore, the temperature of the seal faces is generally higher resulting in steeper thermal gradients. All the friction heat is generated at the seal faces, consequently, the middle portion of the seal face having the longest conduction path must be the hottest. This produces thermal distortion of the radial cross-section of the seal ring and moves the narrowest clearance line towards the middle of the seal face. The warping of the seal face is sufficient to overcome the taper produced by doming of the glass window, otherwise the contact line would remain the same as under stationary conditions; that is at the periphery of the seal face.

In addition, to the distortion of the radial cross-section, there is also a circumferential warping; this forms the basis of a built-in stabilizing mechanism as long as the frictional heat rate remains below the limit value initiating a failure. The self stabilizing mechanism works as follows: some circumferential variations, however small, are always present in seal faces, as well as some misalignment between the faces. Under rotating conditions

the shear rate at the high spots is greater, and local preferential heating results which creates thermal gradients in the seal ring, and seal faces warp tending to accentuate the high spots. At the same time the warping increases the taper of the wedges in the circumferential direction resulting in improved thrust capacity which tends to separate the faces and reduces the frictional heat rate until a compromise is reached resulting in stable operation.

The distortions of the seal faces as discussed above could not be observed directly by interferometric techniques; however, in experimental seals all failure patterns showed a general face geometry as described. Similar failure patterns have also been observed by other investigators[9]. Typical seal face failures at different stages are shown in Figures 5e and 7a, 7b, 7c. All show scoring tracks in the middle of the face. The face of a seal ring after stopping at an early failure stage is shown with the optical flat in Figure 5d. Comparison of fringe patterns with Figure 5c (a typical newly lapped and installed seal ring) shows that the face geometry has no high spots where the wear marks are; thus, the high spots must have been present only while the seal was operating.

Figure 7a shows an incipient failure with two diametrically opposite high spots, while in 7b three unsymmetrically located high spots can be seen. The diametrically opposite high spots were in general most common. This can be explained by the fact that all

experimental seals were carefully lapped and mounted with installation distortions nearly polar symmetric and considerably less than the axial runout Δz. Consequently, the first thermal distortion came at the highest spot due to runout; once this took place the seal face became warped creating the next highest spot diametrically opposite. In a number of failures the two diametrically opposite wear areas were unequal as might be expected on the basis of the above thermal distortion sequence (e.g. Figure 7c).

To reach a stable thermal distortion condition may take considerable time, particularly if the operating conditions are such that the heat removal rate by leakage convection is almost adequate. During test runs a step increase of the closure force produced an increase in the friction torque; after 10 to 20 minutes some of this initial torque increase disappeared. Often the change took even longer showing up as a progressive drift in the friction readings during a particular test setting.

The shifting of the minimum clearance line to the middle of the seal face due to thermal distortion can also explain the slow change in the pressure distribution between seal faces as reported by Mayer[4]. He reports that the slow pressure increase between the seal faces took some 70 minutes to develop and it was assumed to result from hydrodynamic effects of the pressure sensing holes, without an explanation of why it took so long to develop.

3. In the boundary lubrication regime, the closure forces exceed the maximum thrust that can be developed by the thermally distorted seal faces with sealed fluid as lubricant. The seal face distortions are still present as indicated by wear patterns on failed seal faces. Closure force is partly balanced by the thrust bearing effect of the interrupted fluid film and the remainder is carried by direct solid contact. The transition from mixed to boundary lubrication depends on many factors and cannot be related to any particular operating variable. With the experimental glass-carbon seal the transition took place at balance ratios, β, of about 0.6 to 0.7.

In general, boundary lubrication occurs at progressively lower balance ratios with increasing rubbing velocity $\overline{v}$. However, fluid pressure, viscosity, seal runout and particularly seal face geometry are all contributing factors. It was found that boundary lubrication may occur in a given seal at different balance ratios depending on the previous runup history, although fluid temperature, fluid pressure and rubbing velocity are kept the same. The only possible explanation is that starting with a high balance ratio results in different seal face distortions than those produced by a gradual increase of the balance ratio.

It was also found that startup with a high balance ratio could result in seal failures by scoring. On the other hand, stable

operation with the same, and even higher, balance ratios was possible without failure if the closure force was increased slowly, allowing for thermal distortions to build up. This indicates that even in the boundary lubrication regime part of the closure force is carried by the hydrodynamic thrust bearing mechanism. With boundary lubrication the leakage becomes negligible and all the frictional heat must be removed by conduction. As the closure force, i.e. balance ratio, is increased the thrust bearing effect will diminish because of insufficient fluid supply; higher temperatures also contribute by reducing the viscosity of the fluid. An increasing fraction of the closure force will be balanced by direct solid contact pressure and seal faces will eventually fail when the heat generated by friction can no longer be conducted away without exceeding the temperature limitations of the seal materials. Thermal failures occur very rapidly when the boiling temperature of the fluid is reached; as the fluid boils off, friction increases considerably resulting in a sudden heat rate increase producing failure.

For seals operating with boundary lubrication the seal material thermal conductivity, high temperature strength and friction properties are of primary importance. The suitability of materials for mechanical seals has been investigated by Mayer[8]; he evaluates materials in terms of an empirical parameter*.

---

*Wärmespannungsriss-Widerstandsfactor - (Heat stress-tear resistance-factor)

In summary, the two operating regimes of practical interest are the mixed film and the boundary lubrication regimes. In the mixed film regime a mechanical seal operates as a hydrodynamic thrust bearing with a built in stabilizing mechanism based on thermal distortions. There is very little, if any wear, but some leakage is necessary for operation. In the boundary lubrication regime a mechanical seal operates as an overloaded thrust bearing, the excess load being carried by solid rubbing contact between faces. The leakage is reduced to a minimum, but wear rates are higher. Operation at high pressures and high rubbing velocities is not possible with boundary lubrication.

Leakage Rate. Measured leakage rate, Q, plotted against balance ratio, β, for the experimental seal, shows a definite relation between these parameters; Figures 8, 9, 10 and 11.

In the full film and mixed film operating regimes there is exponential dependence between Q and β indicated by a straight line on the log-log plot. The position of the leakage curve differs for different runs with the same seal (without relapping between runs), but the curve is linear and the slope remains practically constant from run to run. The dotted curves in Figures 9 and 10 show results of different test runs with the same seal. In Figure 11 test runs with two different lappings of the seal ring are shown. On a log-log plot the leakage variation is still linear but there is a

difference in the slope in spite of the fact that operating conditions were kept the same and in relapping it was attempted to match the runouts, Δz, as closely as possible.

The maximum Δz values are only the best estimates that could be made using a 0.0001 inch per division dial indicator. In spite of the large percentage errors in Δz measurement, a correlation can be detected between the seal runout and the exponent relating the leakage rate Q with the balance ratio β. The values tabulated below show that the slope of the linear portion of the Q versus β on the log-log plot increases with decreasing runout except for one test run.

n-rpm	maximum Δz inch	slope of Q versus β curve
1600	0.00008	14.6
1000	0.00007	14.7
1800	0.00006	17.7
1800	0.00006	28.6
1300	0.00005	21.6

The high exponent values show that leakage rate Q is extremely sensitive to the balance ratio of the seal; a factor to be remembered in designing mechanical seals.

The rubbing velocity, $\bar{v}$, either has no effect on the leakage rate, or these effects are secondary and are swamped by the high power exponential relation between Q and β.

With boundary lubrication the exponential relationship between

Q and β does not exist; increasing balance ratio will reduce leakage, but at a diminishing rate. Eventually a limiting value of the balance ratio β is reached at which a given seal fails. From the composite of experimental Q versus β curves in Figure 12, it may be seen that, in general, the limiting value of β at failure decreases with the increasing rubbing velocity $\bar{v}$ or rotation speed n; there is no correlation of the failure point with leakage rate or any other variable.

For design and test purposes, Q versus β graphs are useful for determining the transition point from mixed to boundary lubrication regime. By plotting Q versus β, the transition is consistently indicated by the deviation of leakage curve from the straight line on a log-log plot. This enables one to determine the operating regimes of mechanical seals constructed from common engineering materials where visual observation is impossible.

For a given seal, the qualitative changes in leakage rates by changing the seal balance ratio can be predicted on the basis of the experimental data, but there appears to be no way of predicting the quantitative leakage rate.

The dependence between Q and β is exponential with very high exponent values (experimental values 14.6 to 21.6) while in the laminar flow formula, Equation 1, all the variables have only third or lower power effect. Therefore, correlation of leakage on the basis of the laminar flow theory appears unlikely even if an empirical relation can be found relating the clearance z (or an equivalent average value) to fluid pressure P and absolute viscosity η for a given seal type. Before any correlation is attempted considerably more

experimental data is needed.

For sealing efficiency, stable operation in the boundary lubrication regime appears to be the design goal if the reliability can be guaranteed and wear rates are acceptable. Unfortunately, the balance ratio region between the minimum value of β with acceptable leakage rates and the maximum value determined by the failure point becomes narrower with increase in rubbing velocity v and fluid pressure P.

Seal Friction. Values of the friction coefficient, μ, calculated from experimental data are plotted against balance ratio, β, in Figures 12, 13, 14 and 15. There is considerable scatter of points at each test setting and the values of μ obtained with the same seal in different test runs also show wide variation.

Some of the scatter results from experimental errors because all related readings could not be taken simultaneously. In the boundary lubrication regime all torque readings are the best estimates of the average torque under stick-slip conditions. However, the differences in μ values from run-to-run with the same seal without any detectable changes in the seal face cannot result purely from measurement errors; test data is too consistent to indicate errors of such magnitude. The different μ values probably arise from seal face geometry variations due to different runup histories and insufficient stabilization periods before readings were taken.

Considering μ values from different test runs with the same seal (no relapping between runs) under identical conditions, there appears to be a minimum that can be attained at a particular balance

ratio β. Assuming these minimum values to represent the closest approach to the stable operating condition, and allowing for scatter and other experimental errors by statistical averaging, a straight line relationship between μ and β gives the best approximation of experimental results. These best fitting straight lines for different experimental conditions are shown in Figures 12 to 15.

The wide variations of μ-values in the full film regime cannot be readily explained even in terms of relatively large errors in measuring very low torques. It is possible that the seal faces are, in some cases, fully separated resulting in only pure viscous drag, while, in other cases, there is some rubbing contact. In any case this operating region is of little practical interest because leakage rates are unacceptably high for seal applications.

The comparison of μ versus β curves for different speeds is given in Figure 16. The μ values extrapolated along the curves to the β values at failure are indicated by the terminal points of these curves. In general the slope of μ versus β curves is consistently decreasing with increasing rotation speeds n. Friction coefficient values generally show a decrease as the speed increases; however, there is an unexplainable increase of μ values for 1800 rpm test run.

There does not appear to be any correlation of μ values with the seal runout Δz or other operating variables.

Seal Failure. In seal design and applications, the prediction of limiting operation conditions is important. A so-called $P\bar{v}$ - factor or a $\bar{p}\bar{v}\mu$ factor (4) is used by seal manufacturers for this purpose. The $\bar{p}\bar{v}\mu$ - factor is actually a measure of the frictional heat generated per unit face area of a seal.

The measured and extrapolated values of the operating variables and parameters at the failure conditions of the experimental seals are tabulated below.

Test run	No. 24	No. 30	No. 34	No. 39
P - psig	130.4	130.4	130.4	130.4
$\bar{v}$ - fpm	955	1238	1522	1712
β	0.92	0.90	0.833	0.689
μ	0.0162	0.0135	0.011	0.0126
$\bar{p}\bar{v}\mu = \beta P\bar{v}\mu$ ft.lb/in^{2}min	1820	1960	1820	1940
or				
BTU/in^{2}min	2.34	2.52	2.34	2.50

The experimental results show that the failure of a given seal is determined by a limiting friction heat rate. Even though the friction coefficient, μ , values have been extrapolated from curves based on scattered experimental points the agreement of heat rate values at the seal failure point is within eight per cent.

Based on the existing evidence the extrapolated μ values, together with other measured data, permit prediction of failure limits of a given seal design for different combinations of operating variables. This eliminates the need for a large number of failure tests to determine the operating limits for a variety of conditions.

3.5 Evaluation of Experimental Errors.

The gauges used for measuring sealed fluid supply and discharge pressures were calibrated on a dead weight tester. All experimental readings were corrected by using appropriate calibration curves shown in Figure 19. The experimental error in the measured P values results from pressure fluctuations; these could usually be kept within $\pm$ 0.5 psi.

The reading accuracy of the strain-gauge indicator is about $\pm$ 1 μinch/inch and the maximum zero shift of the tie rod strain-gauge bridge circuit during any test run was less than $\pm$ 5 μinch/inch. The corresponding random error in total closure force, F, is $\pm$ 9 pounds.

Thus, the maximum combined random error in the net seal face force, N, is about 13 pounds or less than four per cent of the average N value in the experimental range. The maximum error of four per cent also applies to the average face pressure, $\overline{p}$, and balance ratio, β, values.

The random errors in torque measurements are considerably larger. The reading accuracy of the strain-gauge indicator is the

same but zero shifts of the torque strip strain-gauge bridge of $\pm$ 4 μinch/inch result in higher relative error because stresses in the torque strips were considerably lower. The combined random error in shear force, S, is about 0.2 pound or as much as ten per cent of the lowest shear forces in the experimental range. In the mixed film and boundary lubrication operating regimes the error is generally less than five per cent. With boundary lubrication the stick-slip effects made strain-gauge readings difficult, introducing some additional error which is hard to estimate. However, this error does not appear significant because there is no apparent increase in the scatter of corresponding experimental points on μ versus β graphs.

The shear force error of five to ten per cent is applicable also to the friction coefficient values. Although this random error is appreciable, it is small compared to the changes in the friction coefficient caused by the seal face geometry variations discussed in preceding sections. Unfortunately, there is no way of estimating or predicting these effects on the basis of limited data.

The rotation speed variations were kept within $\pm$ 6 rpm at any one setting. Combined with the reading accuracy of the strobotach of $\pm$ 2 rpm the total random error in n and $\bar{v}$ values is less than one per cent.

The agreement of the limiting friction heat rates calculated from extrapolated friction values is remarkably close and should be substantiated by further tests.

3.6 Continuation of Mechanical Seal Investigation.

The results of the first series of tests have provided a good qualitative picture of the fluid film behavior in the clearance of a mechanical seal. The sealing mechanism has been explained and substantiated by experimental data.

To provide useful quantitative design information the operating and the design variables must be next investigated systematically over a broad range. The following is the proposed program for continuation of the experimental work:

1. Investigation of the major operating variables, without changing seal geometry and size.

   a. With P constant, preferably at 130 psig, conduct experimental runs at speeds below 1000 rpm to cover β values up to at least 1.2 before failure. This would extend the experimental data well into the region of unbalanced seals where $\bar{p} > P$. A six inch diameter spindle pulley will be needed to extend the speed range.

   b. Investigate low pressure operation with P constant in the 40 psig range choosing rotation speeds to produce failures in the β range of 0.7 to 1.2. This will require speeds in excess of 1800 rpm and a larger motor pulley will be needed to extend the speed range.

c. Investigate high pressure operation with P constant in the 450 psig range, again choosing rotation speeds to produce failures in the same β range. It may be necessary to extend the lower speed limit further in order to operate at high β values without failure.

d. Additional photographic work and interferometric measurements can be carried out simultaneously with the collection of numerical data if and when a high intensity monochromatic light source becomes available. Some infrared photography techniques can also possibly be developed to record the temperature distribution in the face of a running seal.

e. At any stage of the experimental work the investigation of transient effects can be undertaken. This requires some additional instrumentation and additional manpower in order to take simultaneous readings of related operating variables.

2. Investigation of the design variables preferably with the same operating pressures as in the preceding tests.

a. Select test runs from previous investigations with extreme values of runouts Δz. Repeat some test runs under identical conditions with seal rings specially lapped to produce opposite extremes in the runouts Δz. Data from the first few runs should indicate

if more extensive testing is needed to pinpoint the effects of runout.

b. Reduce the stiffness of the seal ring by narrowing the radial section to the width of the seal face. Determine the runout as closely as possible and select operating conditions to match some previous test runs with identical runout. If the first tests show significant effects the stiffness of the seal ring can be further varied by changing the height of the cross-section. For thinner rings lapped spacers can be readily made to fit onto the seal adapter. To increase the stiffness a new seal adapter will be needed to accommodate a thicker seal ring.

c. Decrease the face width b of the seal rings to about 1/16 inch keeping the average diameter, $\bar{D}$, constant. Conduct the first test runs under operating conditions to match the runout values of previous tests.

d. Prepare seals with circumferential waviness of a few lightbands in the face. This can be done by "fingering" a flat lapped seal surface with fine abrasive. The number of high spots around the circumference should be at least three. Matching the operating conditions with a previously tested flat lapped seal with

equal runout would permit detection of any significant increase of thrust capacity.

e. Operation in the mixed regime depends largely on adequate lubricating fluid supply to maintain the thrust bearing effect. Rotating seal rings with noncircular face boundaries on the pressure side have been tried in some seal designs to improve lubrication of the seal faces. Visual observation of the interface fluid film allows direct evaluation of such seal designs.

3. Investigation of seal materials and cooling effects.

a. The glass window can be readily replaced by properly finished plates of different materials. With adequate data from preceding tests the operating regime can be predicted from leakage rate plots without the need for visual observation. The incipient failure should be indicated by abrupt torque increases, similar to those observed in glass-carbon seal tests. Tests using different material pairs can be conducted to provide useful design information such as friction coefficients and limiting heat rates.

b. Common engineering materials are readily machinable to provide cooling for temperature control of the seal plate which replaces the window, or its upper

surface. Connections can be readily built into the mounting ring assembly without disturbing other parts of the apparatus. The instrumentation for temperature and direct sealed pressure measurement can also be easily adapted once the transparent glass window is traded for machinable material.

The proposed program has been set up on the assumption that experimental data obtainable with the existing apparatus is collected and studied first. The next steps would involve only minor modifications such as extending the speed range and increasing the power available from the spindle drive. The more complicated experiments to provide answers to specific design problems could then be planned by taking advantage of all the accumulated test data.

3.7 Conclusions.

1. The faces of a mechanical seal although initially lapped flat are elastically distorted by installation stresses. These distortions have at least the same order of magnitude as the currently accepted flatness standards for lapped seal faces.

2. With a stationary mechanical seal, the zero leakage condition requires a continuous solid-to-solid line contact around the seal face. In order to have this contact the closure force must be sufficiently big to overcome the installation distortions and misalignments that are present in every seal.

3. Under operating conditions the thermal distortions of the seal faces are significant. They perform an essential function in the operating mechanism of a mechanical seal.

4. In a rotating mechanical seal there are two different operating regimes, the mixed film and the boundary lubrication regime, that result in sufficiently low leakage rates to be of practical usefulness.

In the mixed film regime continuous fluid film extends part way into the seal clearance and such a seal operates as a hydrodynamic thrust bearing. The stabilizing mechanism is based on circumferential wedges in the seal clearance produced by thermal distortions.

In the boundary film regime there is no circumferentially continuous fluid film in the seal clearance and a seal operates as an overloaded hydrodynamic thrust bearing. Some fraction of the closure forces is carried by hydrodynamic pressures, the remainder by solid rubbing with boundary lubrication over the contact areas.

5. In the mixed film regime the leakage rate, Q, is a high power exponential function of the balance ratio, β. The value of the exponent depends to some extent on the runout, Δz, of the seal; generally it increases with the diminishing runout. In the experimental seal the exponent values were 14.6 to 21.6 corresponding to runouts of 0.00008 to 0.00005 inches.

6. In the boundary lubrication regime the exponential relationship between Q and β breaks down, and Q decreases at a diminishing rate with increasing β value.

7. Absolute leakage rate does not depend on the balance ratio alone. It is a function of many variables. One of the important variables is the transient operating history from startup to the particular stable condition; this influences the thermal distortions of the seal faces and the resulting clearance geometry.

8. The numerical value of the friction coefficient, μ , for a given seal is a function of several variables; it can be determined with reasonable accuracy only by experiment. However, the value of μ varies linearly with β and can be extrapolated with good accuracy. In general the slope of μ versus β curve decreases with increasing rubbing velocity, $\overline{v}$.

9. The failure point of a given seal is determined by a limiting heat rate. The limiting heat rate for a given seal remains constant over a range of operating conditions and permits prediction of seal failure for different combinations of operating variables. In all the experimental seal failures over a speed range of 1000 to 1800 rpm, the heat rates producing failure agreed within eight per cent.

10. Choice of the mechanical seal operating regime is necessarily a compromise between acceptable leakage and wear rates. The boundary lubrication regime results in the lowest leakage rates

but differential pressures and/or rubbing velocities are limited to low values by allowable wear and heat rates. The mixed film regime requires some continuous leakage, but properly designed seals can be operated at high differential pressures and rubbing velocities with very little wear. For reliable operation the balance ratio must be closely controlled.

11. In order to formulate a meaningful theory to be used as a design basis, a realistic mathematical model is needed. The steady state clearance geometry depends on the previous operating history, therefore the transient effects must be known or at least controllable in practice. Existing experimental data indicate that in the basic fluid flow equations the standard simplifying assumptions, such as constant viscosity, temperature and suitably prescribed boundary conditions, cannot be made. Under such conditions any mathematical treatment becomes extremely difficult.

If simplifying assumptions must be made in order to make the analysis tractable, there must be sufficient experimental data to justify such assumptions, otherwise the analysis becomes academic and is of little use.

12. At the present stage, the most fruitful course for further investigation appears to be systematic experimental investigation to find the effect of operating and design variables. Adequate numerical data for a future analytical approach may then appear.

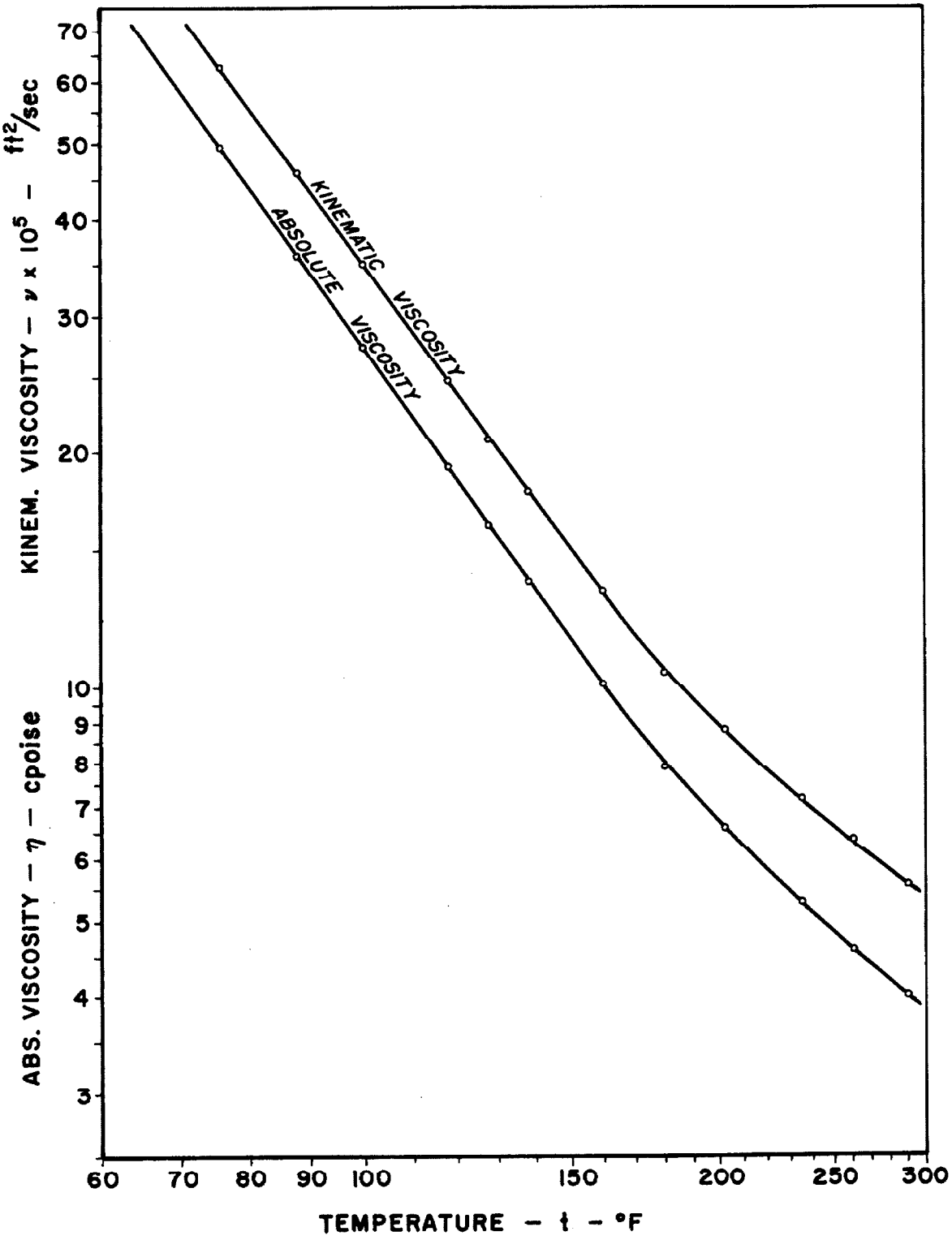

Figure 18. Temperature-viscosity curves for the hydraulic oil used in seal tests.

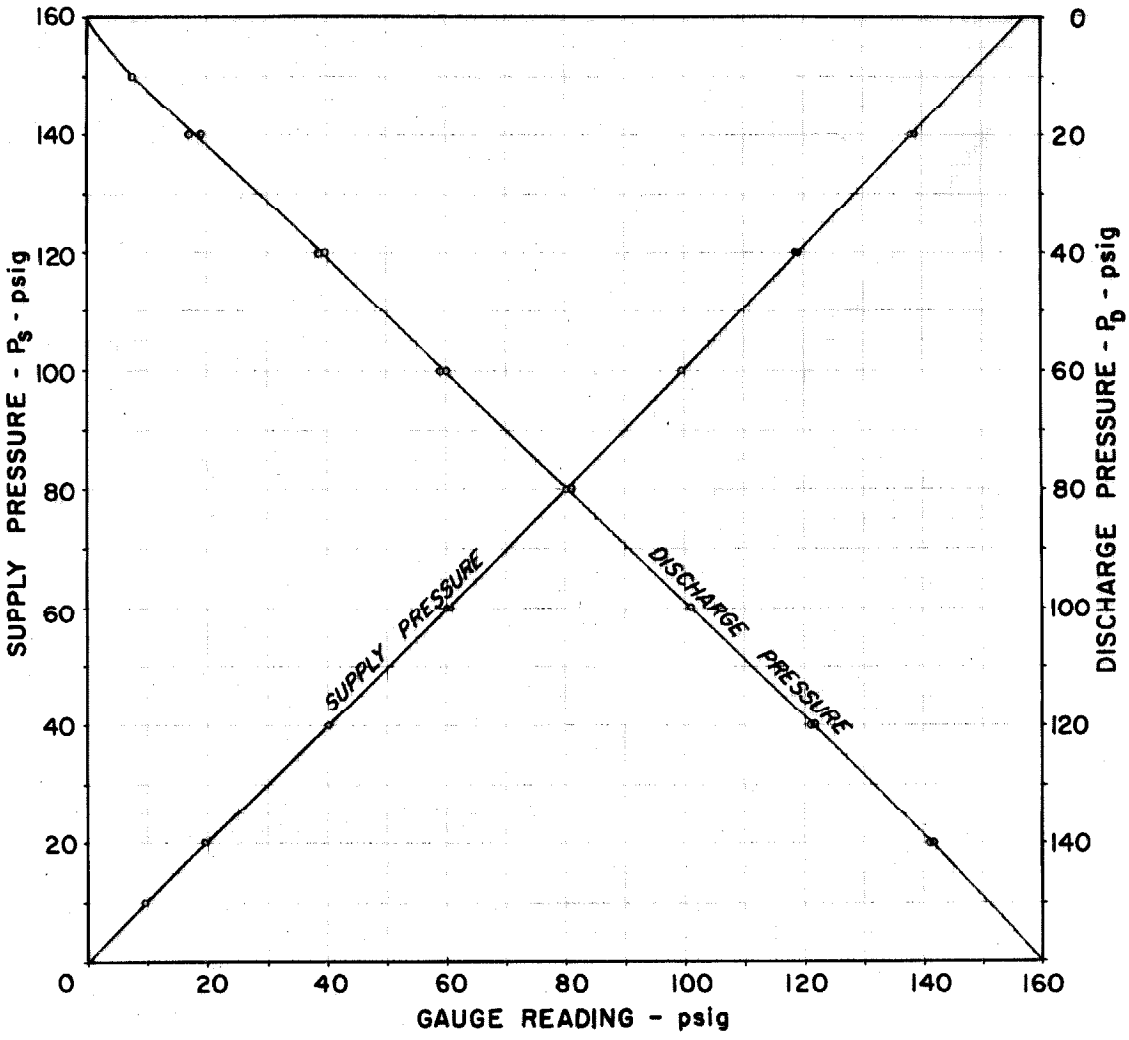

Figure 19. Calibration curves for the supply and the discharge pressure gauge.

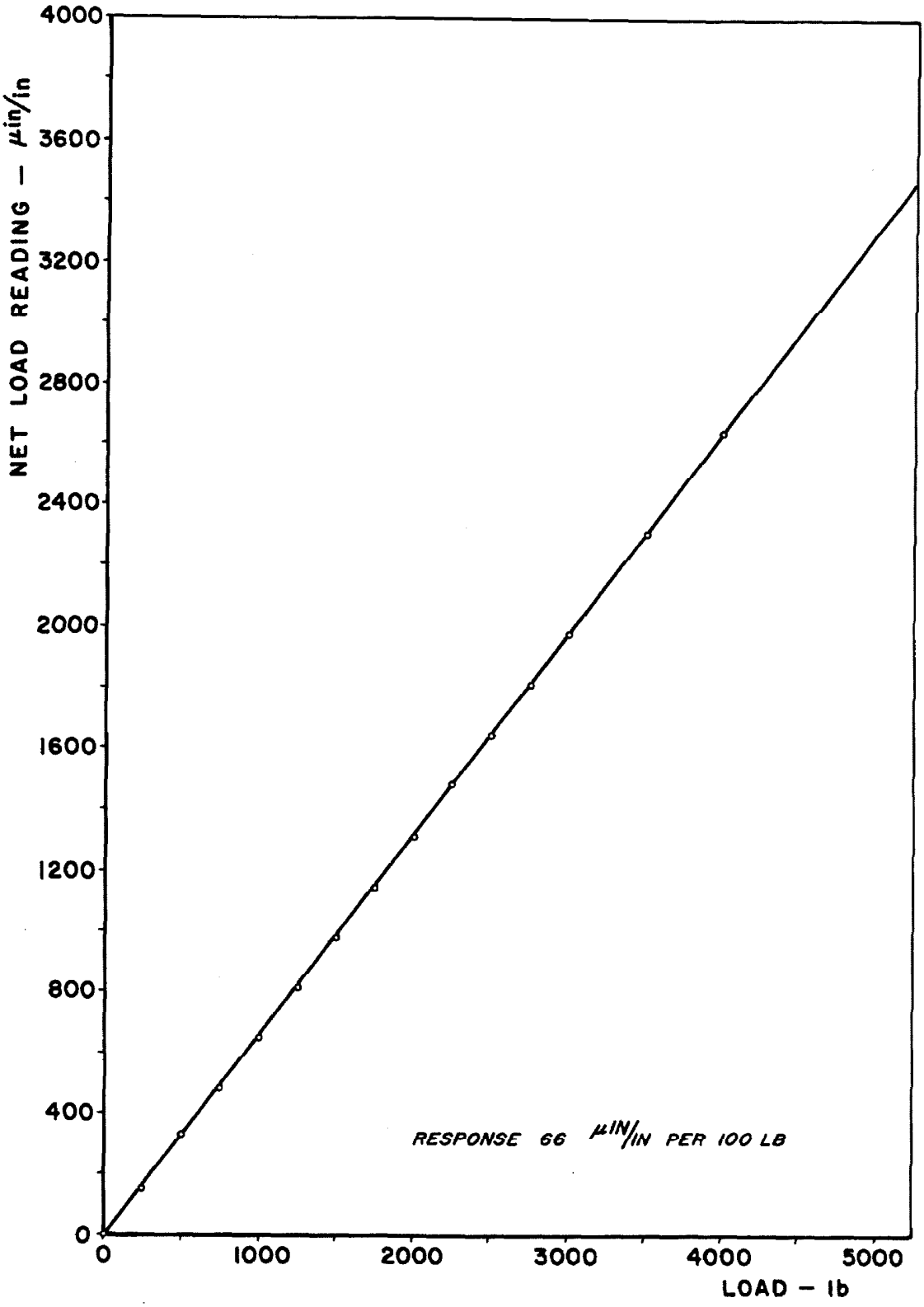

Figure 20. Calibration curve for the tie rod strain gauge bridge.

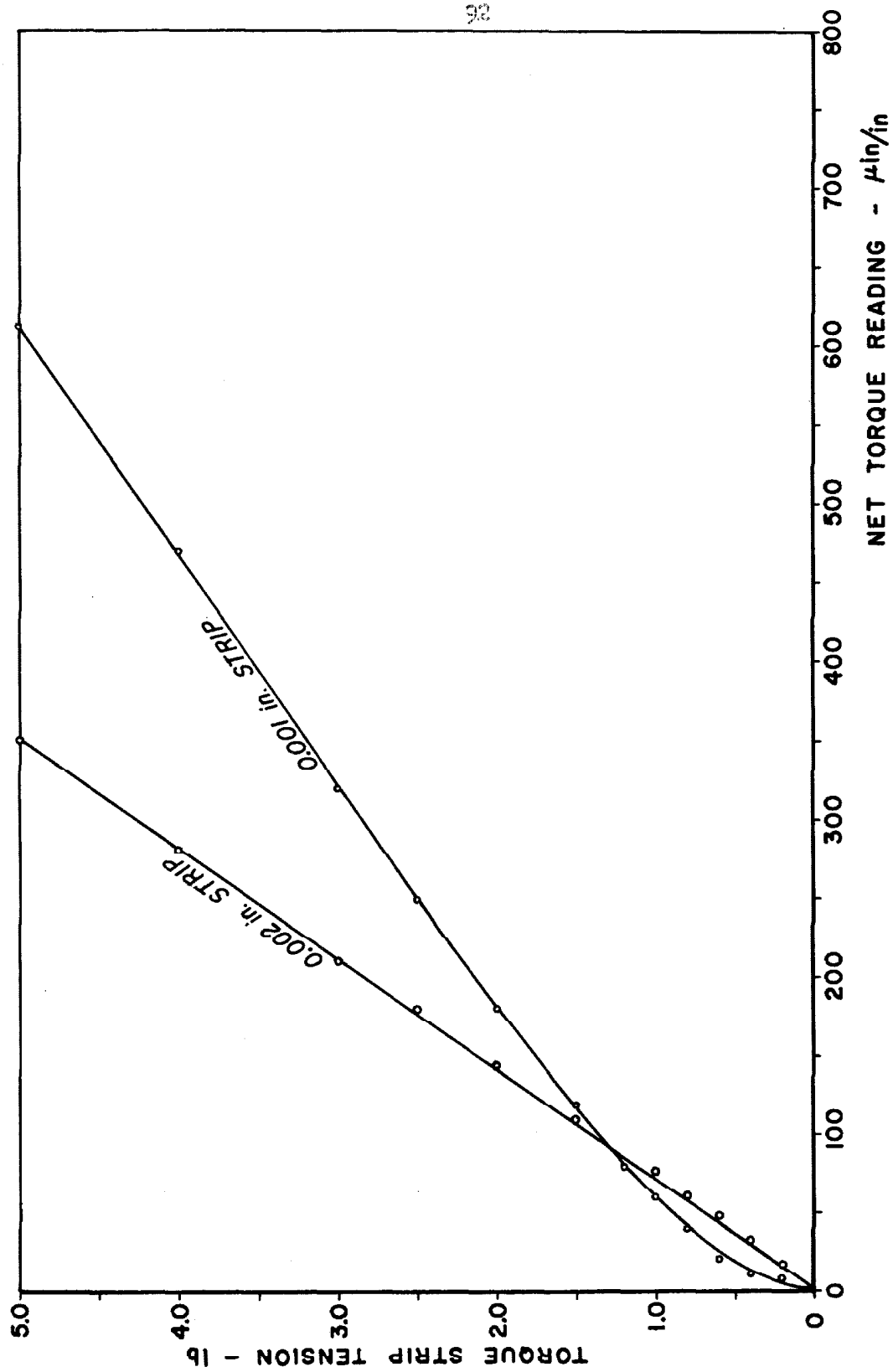

Figure 21. Calibration curves for the torque strip strain gauge bridges.

REFERENCES

1. "Stuffingbox for Refinery Pumps Packing vs. Mechanical Seal," A. Hollander, California Oil World and Petroleum Industry, Second issue, March 1944.

2. "The Mechanical Seal -- Its Construction, Application and Utility," C. E. Schmitz, ASME Trans., 1949, p. 635.

3. "Boundary Film Investigations," S. J. Needs, ASME Trans., 1940, Vol. 62, p. 331-345.

4. "Leakage and Wear in Mechanical Seals," E. Mayer, Machine Design, Vol. 32, March 3, 1960, p. 106-113.

5. "Effect of Environmental Control on Mechanical Seal Success," R. E. Morgan, ASME - Paper 63-WA-259, November 1963 Meeting, 5 p.

6. "Materials in End-Face Mechanical Seals," K. Schoenherr, ASME - Paper 63-WA-254, November 1963 Meeting, 9 p.

7. "Experimental Investigation of Oil-Film Behavior in Short Journal Bearings," B. Auksmann, ASME - Paper 61-LUB-11, October 1961.

8. "Das Widerstandsvermögen von Gleitwerkstoffen Axialer und Radialer Gleitringdichtungen gegen Wärmespannungsrisse," E. Mayer, VDI Zeit., Vol. 102, June 21, 1960, p. 728-732.

9. "Development in the Uses of Radial Face Mechanical Seals for Gas Sealing Applications," S. C. W. Wilkinson, British Hydromechanical Research Association International Conference on Fluid Sealing, April 1961, Paper C3.

10. "Some Notes on Seals for Rotating Shafts," E. F. Boon, S. Honingh, D. C. Van Rijssen, Proceedings of Fourth World Petroleum Congress, 1955, Sect. VII/A, p. 9-11.

11. "Mechanical Shaft Seals in Chemical Industry," T. H. Wood, Institute of Chemical Engineers Transactions, Vol. 32, No. 1, 1954, p. 73-80.

12. Modern Interferometry, C. Chandler, p. 76, Hilger and Watts, Ltd. 1951.

13. "Rotating Seals for High Pressure," H. F. Greiner, Product Engineering, Vol. 27, February 1956, p. 140-143.

14. "Mechanical Seals," J. C. Mason, Plant Engineering, Vol. 13, April 1959, p. 123-127.

15. "Face Type Rotating Shaft Seals -- How to Use Them," J. Riddle, R. D. Durrett, Mill and Factory, Vol. 63, September 1958, p. 87-90.

16. "Developing Face Seals for Rotating Shafts," M. G. Marsh, Nuclear Engineering, Vol. 7, April 1962, p. 149-151.

17. "Use of Carbon-Graphite in Mechanical Seals," W. R. Lauzau, B. R. Shelton, R. A. Waldheger, Lubrication Engineering, Vol. 19, May 1963, p. 201-209.

18. "Mechanical Seals in Pumps for Hydronic Systems," R. W. Janetz, Lubrication Engineering, Vol. 19, August 1963, p. 321-326.

19. "Select Best Pump Seal," H. E. Tracy, Chemical Engineering, April 1957, p. 239-254.

20. "Inquiry Specifications for Mechanical Seals," T. W. Hudson, ASME - Paper 63-WA-203, November 1963 Meeting, 5 p.

21. "Testing High Speed Seal Carbons," R. R. Paxton, W. R. Shobert, ASLE Transactions, Vol. 5, November 1962, p. 308-314.

22. "End Face Seals in Light Hydrocarbon Liquids," E. W. Conklin, ASME - Paper 63-PET-29, October 1963.

23. "Mechanical Shaft Seals," S. Sussman, Air Conditioning, Heating and Ventilation, Vol. 57, July 1960, p. 61-66.

24. "Basic Principles of Mechanical Seals," T. J. Sniffen, Product Engineering, Vol. 29, September 1958, p. F12-F14.

25. "Testing Carbon for Seals and Bearings," R. R. Paxton, W. R. Shobert, Lubrication Engineering, Vol. 17, January 1961, p. 27-33.

BIBLIOGRAPHY

1. "Carbon-Packing Progress for Sealing Small Turbines," K. MacDonald, Power, Vol. 98, July 1954, p. 122-23, 200, 204.

2. "Gleitringdichtungen fur Drehende Wellen," G. Diefenbach, Chemie-Ingenieur-Technik, Vol 26, July 1954, p. 397-400.

3. "Development in Shaft Seals," Pumping, 5, April 1963, p. 206-8.

4. "Oil Seals for Rotating Shafts," A. R. G. Hewett, Engineering Designer, September 1963, p. 14-18.

5. "Abrasive Resistant Seals; Advantages of Sintered Metal Filter Ring," G. C. Witcombe, B. J. Hillman, Pumping, 5, October 1963, p. 563-5.

6. "Mechanical Seal Design," S. C. W. Wilkinson, Engineering Materials and Design, 5, pt. 1, August 1962, p. 572-6; pt. 2, September 1963, p. 664-7.

7. "Introduction to Mechanical Seals," A. R. G. Hewett, Engineering Designer, May 1962, p. 3-5.

8. "Principles of Gas-Lubricated Shaft Seals," S. Whitley, L. G. Williams, Journal of Mechanical Engineering Science, 4, June 1962, p. 117-87.

9. "Testing Mechanical Seals at Crane Packing, Ltd.," British Petroleum Equipment News, 9, Autumn 1962, p. 56-8.

10. "How to Maintain Mechanical Seals," T. E. Alexander, Oil and Gas Journal, Vol. 60, February 12, , p. 123-4, 127.

11. "Friction and Wear for Wafer-Lubricated Seals," R. L. Cornell, R. S. Lucas, H. L. Young, Product Engineering, Vol. 32, July 24, 1961, p. 38-41.

12. "Some Recent Results in Fluid Sealing Research," B. S. Nau, International Fluid Power Conference Proceedings 1962, p. 81-90.